

Severe Acute Respiratory Syndrome Coronavirus Papain-like Novel Protease Inhibitors: Design, Synthesis, Protein–Ligand X-ray Structure and Biological Evaluation[†]

Arun K. Ghosh,^{*,‡} Jun Takayama,[‡] Kalapala Venkateswara Rao,[‡] Kiira Ratia,[§] Rima Chaudhuri,[§] Debbie C. Mulhearn,[§] Hyun Lee,[§] Daniel B. Nichols,[‡] Surendranath Baliji,[‡] Susan C. Baker,[‡] Michael E. Johnson,[§] and Andrew D. Mesecar[§]

[‡]Departments of Chemistry and Medicinal Chemistry, Purdue University, 560 Oval Drive, West Lafayette, Indiana 47907, [§]Center for Pharmaceutical Biotechnology and Department of Medicinal Chemistry and Pharmacognosy, University of Illinois at Chicago, 900 S. Ashland, Chicago, Illinois 60607, and [‡]Department of Microbiology and Immunology, Loyola University of Chicago, Stritch School of Medicine, Maywood, Illinois 60153

Received April 12, 2010

The design, synthesis, X-ray crystal structure, molecular modeling, and biological evaluation of a series of new generation SARS-CoV PLpro inhibitors are described. A new lead compound **3** (6577871) was identified via high-throughput screening of a diverse chemical library. Subsequently, we carried out lead optimization and structure–activity studies to provide a series of improved inhibitors that show potent PLpro inhibition and antiviral activity against SARS-CoV infected Vero E6 cells. Interestingly, the (*S*)-Me inhibitor **15h** (enzyme IC₅₀ = 0.56 μM; antiviral EC₅₀ = 9.1 μM) and the corresponding (*R*)-Me **15g** (IC₅₀ = 0.32 μM; antiviral EC₅₀ = 9.1 μM) are the most potent compounds in this series, with nearly equivalent enzymatic inhibition and antiviral activity. A protein–ligand X-ray structure of **15g**-bound SARS-CoV PLpro and a corresponding model of **15h** docked to PLpro provide intriguing molecular insight into the ligand-binding site interactions.

Introduction

Severe acute respiratory syndrome (SARS^a) was first reported in Guangdong province, China, in November 2002.¹ SARS is a contagious respiratory illness with no effective treatment to date. SARS affected three continents, infecting more than 8000 individuals and causing nearly 800 deaths. Fortunately, the spread of SARS-CoV was contained after the initial outbreaks through public health measures. As it turned out, the etiological agent of SARS is a novel coronavirus, SARS-CoV.^{2,3} There have been no known new cases of SARS since 2005. However, recent isolation of strains from zoonotic origins thought to be the reservoir for SARS-CoV raises the possibility of a reemergence of SARS and related ailments.^{4,5} Consequently, design and development of antivirals effective against SARS-CoV should be an important priority against future outbreaks.

Biochemical events critical to the viral replication revealed a number of important targets for therapeutic intervention of SARS.^{6,7} Most notably, two cysteine proteases, a papain-like protease (PLpro) and a 3C-like protease (3CLpro), play a critical role in the virus-mediated RNA replication. Not surprisingly, numerous studies related to the development of SARS-CoV 3CLpro inhibitors have already been reported.^{8,9} In contrast, very few inhibitor design efforts against SARS-CoV PLpro have been reported. We recently reported the

discovery and design of a series of unprecedented noncovalent SARS-CoV PLpro inhibitors displaying antiviral activity against SARS-CoV with no associated cytotoxicity.¹⁰ Subsequently, a protein–ligand X-ray structure provided important molecular insights for further design and optimization of inhibitors.¹⁰ This initial work demonstrated that PLpro is a viable target for the development of anti-SARS therapeutics.

Besides viral peptide cleavage, recent structural and functional studies demonstrated that PLpro is involved in a number of other important biochemical events, such as deubiquitination, deISGylation, and involvement in the virus evasion from the innate immune response.^{11,12} The homologous enzyme PLP2, from the human coronavirus 229E, has been shown to be critical to 229E viral replication.¹³ In addition, recent studies have shown that human deubiquitinating enzymes are potential anticancer drug-design targets. Thus, PLpro is a significant target for development of drugs against SARS and is a model for development of drugs against other deubiquitinating enzymes involved in human diseases.

Recently, our primary screening of a library of 50 080 diverse, druglike compounds led to the identification of two compounds after lead validation. Both leads reproducibly inhibited PLpro in a dose dependent manner in the absence and presence of Triton-X. Subsequently, our optimization efforts of the most potent lead, **1** (7724772), containing a benzamide scaffold (IC₅₀ = 20.1 ± 1.1 μM) led to the design of novel PLpro inhibitor **2** and related derivatives that displayed antiviral activity against SARS-CoV. We recently reported a detailed study describing synthesis, biological studies, and X-ray structure of the protein–ligand complex of **2**-bound PLpro.¹⁰ In our continuing studies toward the development of noncovalent/reversible PLpro inhibitors, we

[†]The PDB accession code for **15g**-bound PLpro X-ray structure is 3MJ5.

*To whom correspondence should be addressed. Phone: (765) 494-5323. Fax: (765) 496-1612. E-mail: akghosh@purdue.edu.

^aAbbreviations: SARS, severe acute respiratory syndrome; SARS-CoV, severe acute respiratory syndrome coronavirus; 3CLpro, chymotrypsin-like protease; PLpro, papain-like protease; WHO, World Health Organization.

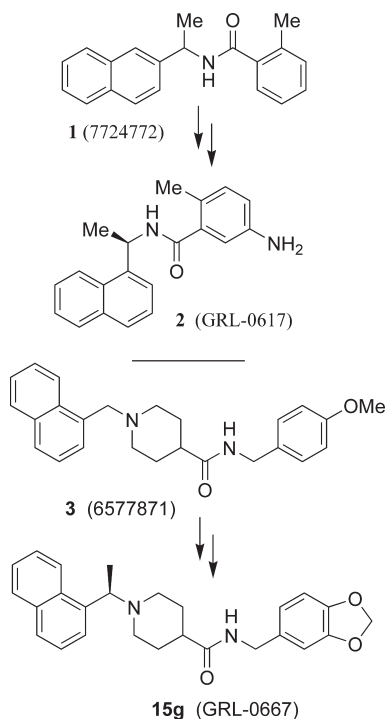


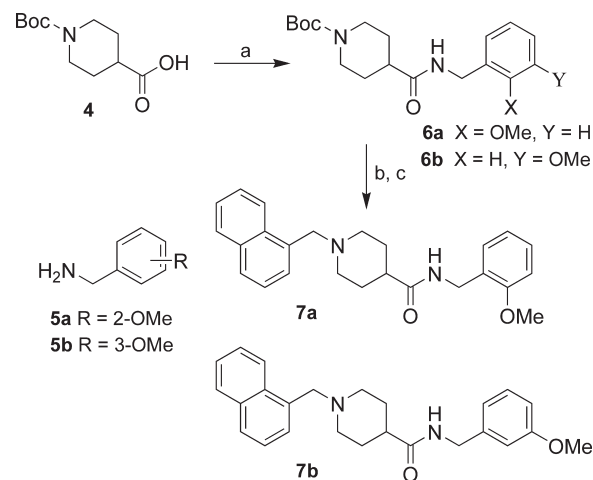
Figure 1. Structures of PLpro inhibitors **1–3** and **15g**.

have now investigated the potential of the second and less potent lead that evolved from our high-throughput screening efforts. The second HTS lead, compound **3** (Figure 1), contains a piperidine carboxamide scaffold and exhibited an IC_{50} value of $59 \mu M$. Our subsequent lead optimization efforts led to the design of potent inhibitor **15g** ($IC_{50} = 0.32 \mu M$) which inhibited SARS-CoV viral replication in Vero cells with an EC_{50} value of $9.1 \mu M$. The corresponding enantiomer **15h** has shown slightly less potent enzyme inhibitory activity ($IC_{50} = 0.56 \mu M$) and similar antiviral potency. A protein–ligand X-ray structure of **15g**-bound SARS-CoV PLpro was determined. Interestingly, this structure revealed a unique mode of binding with SARS-CoV PLpro and that key molecular interactions of inhibitor **15g** are quite different from the active-site interactions with inhibitor **2**. Herein we describe the design, synthesis, structure–activity studies, molecular modeling, protein–ligand X-ray structure, and biological evaluation of a series of novel and noncovalent inhibitors of SARS-CoV PLpro.

Chemistry

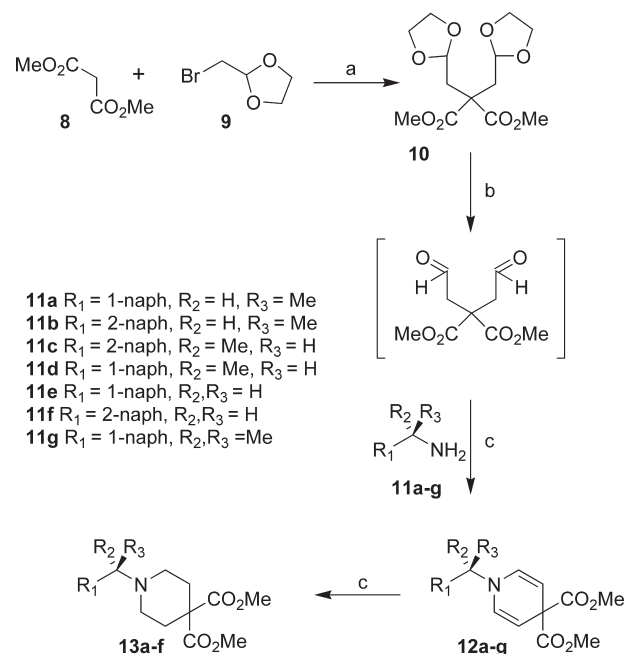
To ascertain the importance of the position of the methoxy substituent in lead inhibitor **3**, we have synthesized the corresponding 2-methoxy and 3-methoxybenzyl derivatives. As shown in Scheme 1, Boc-piperidine-4-carboxylic acid **4** was coupled with 2- and 3-methoxybenzylamines **5a** and **5b** using *N*-(3-dimethylaminopropyl)-*N'*-ethylcarbodiimide hydrochloride (EDCI) and 1-hydroxybenzotriazole hydrate (HOBT) in the presence of *N*-methylmorpholine (NMM) in CH_2Cl_2 to provide coupling products **6a** and **6b** in 92% and 94% yield, respectively. Removal of Boc-group by exposure to trifluoroacetic acid (TFA) in CH_2Cl_2 at $0–23 \text{ }^\circ C$ for 6 h afforded the respective amine. Reductive amination of these amines with 1-naphthaldehyde using $Na(OAc)_3BH$ in the presence of acetic acid furnished inhibitors **7a** and **7b** in 70% and 71% yield, respectively.

Scheme 1^a



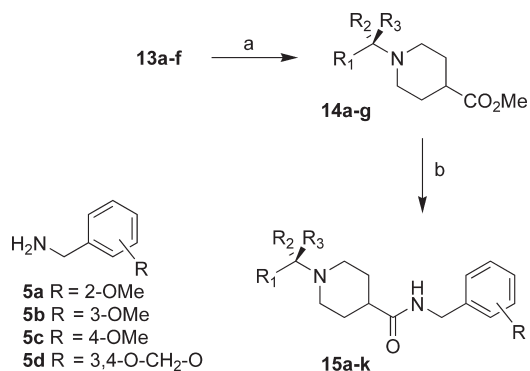
^a Reagents and conditions: (a) **5a** or **5b**, EDCI, HOBT, NMM, CH_2Cl_2 , $23 \text{ }^\circ C$, 5 h; (b) TFA, $0–23 \text{ }^\circ C$, 6 h; (c) 1-naphthaldehyde, $Na(OAc)_3BH$, AcOH, CH_2Cl_2 , $23 \text{ }^\circ C$, 12 h.

Scheme 2^a

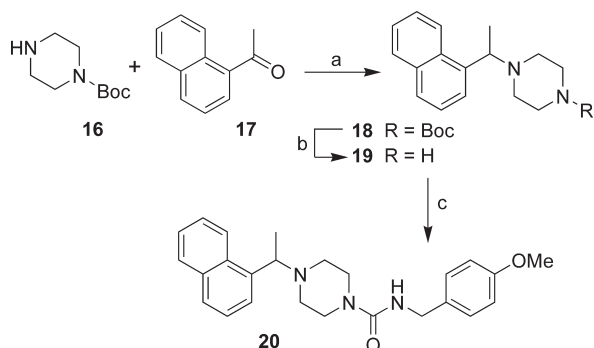


^a Reagents and conditions: (a) KO^tBu , DMSO, $23 \text{ }^\circ C$, 48 h; (b) 10% HCl, THF, $23 \text{ }^\circ C$, 18 h; (c) $NaHCO_3$, $23 \text{ }^\circ C$, 16 h; (c) H_2 , PtO_2 , EtOAc, $23 \text{ }^\circ C$, 2 h.

For structure–activity studies and optimization of potency, we planned to synthesize derivatives of both 1- and 2-naphthylethylpiperidin-4-carboxylic acids and coupled them with various substituted benzylamine derivatives. The synthesis of substituted piperidine-4-carboxylic acids is shown in Scheme 2. Alkylation of dimethyl malonate **8** with commercially available 2-bromomethyl-1,3-dioxolane **9** in the presence of KO^tBu in DMSO at $23 \text{ }^\circ C$ afforded malonate derivative **10** as described previously.¹⁴ Deprotection of the ketal functionalities was carried out by treatment of **10** with 10% aqueous HCl in THF at $23 \text{ }^\circ C$. The reaction was quenched with solid $NaHCO_3$, and the resulting crude dialdehyde was used directly for the subsequent condensation reaction. Condensation of the dialdehyde with various

Scheme 3^a

^a Reagents and conditions: (a) NaCN, DMF, reflux, 16 h; (b) LiOH·H₂O, THF/MeOH/H₂O (3:1:1), 23 °C, 16 h; (c) **5a-d**, EDCI, HOBT, DIPEA, CH₂Cl₂/DMF (9:1), 23 °C, 15 h.

Scheme 4^a

^a Reagents and conditions: (a) NaBH₃CN, MeOH/AcOH (50:1), 23 °C, 48 h; (b) TFA, CH₂Cl₂, 23 °C, 2 h; (c) **5c**, *N,N'*-carbonyldiimidazole, CH₂Cl₂, 23 °C, 4 h.

optically active (*S*)- and (*R*)-1-methyl-1-naphthylmethylamines, 1-methyl-2-naphthylmethylamines, 2-naphthylmethylamine, 1-naphthylmethylamine, and dimethyl-1-naphthylmethylamine **11a-g**¹⁰ in aqueous THF for 16 h afforded dihydropyridines **12a-g** in 39–62% yield.^{15,16} Catalytic hydrogenation of dihydropyridines **12a-f** in ethylacetate at 23 °C provided various piperidine derivatives **13a-f** in 60–94% yield.

The synthesis of various test inhibitors is shown in Scheme 3. Treatment of diesters **13a-f** with NaCN in DMF at reflux for 16 h provided methyl esters **14a-f** in 38–92% yield. Dihydropyridine derivative **12g** was similarly converted to methyl ester **14g** in a two-step sequence. Saponification of **14a-g** with aqueous LiOH in a mixture (3:1:1) of THF, methanol, and water at 23 °C for 16 h afforded the corresponding carboxylic acids. Coupling of these resulting carboxylic acids with benzylamine derivatives **5a-d** utilizing EDCI in the presence of diisopropylethylamine as described above furnished various inhibitors **15a-k** in excellent yield (80–99%).

To evaluate the effect of the corresponding piperazine derivatives, we sought to synthesize racemic piperazine derivative **20**, and the synthesis is outlined in Scheme 4. Reductive amination¹⁷ of Boc-piperazine **16**¹⁸ with 1-acetonaphthone **17** using sodium cyanoborohydride in a mixture (50:1) of methanol and acetic acid at 23 °C for 48 h afforded **18** in 24% yield. Removal of the Boc-group by treatment with trifluoroacetic acid in CH₂Cl₂ at 23 °C for 2 h provided amine **19**.¹⁹ Treatment

Table 1. Structure and Activity of 1- and 2-Naphthylmethyl Derivatives^a

Compound	Structure	IC ₅₀ (μM)
3		59.2 ± 7.8
7a		116 ± 30
7b		30 ± 3
15a		1.21 ± 0.04
15b		0.34 ± 0.01
15c		0.34 ± 0.01
15d		13.2 ± 0.6
15e		34.8 ± 4.0
15f		5.8 ± 0.1
20		>100

^a NA = not active.

of 4-methoxybenzylamine **5c** in the presence of *N,N'*-carbonyldiimidazole in CH₂Cl₂ followed by addition of **19** and stirring of the resulting mixture at 23 °C for 4 h afforded piperazine derivative **20** in 90% yield.

Results and Discussion

The second HTS lead **3** is considerably weaker than the first lead inhibitor **1**, a benzamide derivative of 2-naphthylethylamine. To enhance activity, we first investigated the effect of 2-methoxy and 3-methoxy derivatives **7a** and **7b** on PLpro inhibitory activity. As shown in Table 1, 2-methoxy derivative **7a** showed a very poor inhibitory activity. The 3-methoxy

derivative, **7b**, however, displayed slightly better activity than the starting lead **3**. Our previous structure–activity of lead **1** established that 1-naphthylethylamides were significantly more potent than the corresponding 2-naphthyl derivative. The X-ray structure of **2** bound to PLpro demonstrated that a (*R*)-1-naphthylethylamide forms hydrophobic interactions with the Tyr-265 and Tyr-269 aromatic rings and with side chains of Pro-248 and Pro-249.¹⁰ The preference for (*R*)-methyl was also documented, as it points into the interior of the enzyme between Tyr-265 and Thr-302. On the basis of this ligand-binding site interaction, we elected to incorporate the (*R*)-methyl group. As shown in Table 1, the (*R*)-methyl derivative **15a** displayed an IC₅₀ value of 1.2 μM. To ascertain the importance of the position of the methoxy group, we synthesized *m*-methoxy and *p*-methoxy derivatives. Interestingly, *m*-methoxy derivative **15b** exhibited improvement of enzyme inhibitory activity with an IC₅₀ value of 0.34 μM. The corresponding *p*-methoxy derivative **15c** has also shown similar potency enhancement (> 170-fold over **3**). However, the 2-methoxy derivative **15a** showed a 3-fold reduction in potency over **15b** and **15c**. We then examined the effect of 2-(*R*)-naphthylethyl derivatives on potency. As shown, both *m*-methoxybenzylamide **15d** and *o*-methoxybenzylamide **15e** displayed significant reductions in potency compared to the 1-(*R*)-naphthylethyl derivatives **15b** and **15a**, respectively. Interestingly, the 2-(*S*)-naphthylethyl derivative **15f** is 2-fold more potent than the 2(*R*)-derivative **15d**.

We next examined the effect of a piperazine ring in place of piperidine in **15c** by preparing compound **20**. However, this piperazine derivative showed no activity against PLpro. Most likely, the piperazine derivative showed no activity against PLpro because of the structural constraints imposed by the carbon to nitrogen replacement on this ring. The new nitrogen is then attached to the amide group, forming a urea moiety. This urea moiety will tend to be planar, imposing a flexibility constraint. GOLD docking shows the amide to rotate ~90° away from the optimal hydrogen-bonding orientation (data not shown) of the other active compounds described here.

Our structure–activity studies established that both *m*-methoxy and *p*-methoxy derivatives (**15b** and **15c**) are equally potent. Our preliminary modeling studies indicated that either methoxy oxygen (meta or para) is within proximity to form a hydrogen bond with the Gln-270 carboxamide side chain. On the basis of these possible interactions, we incorporated a benzodioxolane ring and examined its effect on inhibitory potency. As shown in Table 2, dioxolane derivative **15g** exhibits potency comparable to the corresponding *m*- and *p*-derivatives **15b** and **15c**. The corresponding (*S*)-derivative **15h** also shows comparable enzyme inhibitory activity. To examine the preference for a methyl group over a hydrogen at the 1- and 2-naphthylmethyl positions, we have synthesized and evaluated the corresponding unsubstituted derivatives **15i** and **15j**. As shown, both compounds displayed significant reduction in potency, indicating the importance of the methyl group. We have also examined the corresponding *gem*-dimethyl derivative **15k**. Interestingly, this compound is inactive, indicating that both methyl groups cannot be accommodated by the PLpro active site.

Antiviral activities of selected PLpro inhibitors were determined, and the results are shown in Table 3. The compounds were assayed for their ability to rescue a Vero cell culture from SARS-CoV infection. The viability of virus-infected Vero E6 cells as a function of inhibitor concentration was measured relative to mock-infected cells using a luminescence assay.

Table 2. Structure and Activity of Benzodioxolane Derivatives

Compound	Structure	IC ₅₀ (μM)
15g		0.32 ± 0.01
15h		0.56 ± 0.03
15i		~ 45
15j		~ 100
15k		>200

Table 3. Evaluation of Compounds as Inhibitors of SARS-CoV Replication in a Cell-Based Assay

compd	IC ₅₀ (μM)	EC ₅₀ (μM)
3	59.2 ± 7.8	NI
15a	1.21 ± 0.04	11.6 ± 0.6
15b	0.34 ± 0.01	9.7 ± 0.3
15c	0.34 ± 0.01	10.2 ± 0.5
15f	5.8 ± 0.1	> 25
15g	0.32 ± 0.01	9.1 ± 0.5
15h	0.56 ± 0.03	9.1 ± 0.3

This protocol allows for the evaluation of both inhibitor efficacy and cytotoxicity. As can be observed from the data presented in Table 3, the original HTS lead (**3**) does not show any antiviral activity. However, all 2-, 3-, and 4-methoxy derivatives **15a–c** show comparable antiviral activity. Inhibitor **15f** with a 2-naphthyl substituent displayed no antiviral activity. While the (*R*)-methyl derivative **15g** showed slightly better enzyme activity than the (*S*)-methyl derivative **15h**, both inhibitors exhibited the same antiviral potency (EC₅₀ = 9.1 μM). Interestingly, both dioxolane derivatives **15g** and **15h** showed antiviral activity approximately comparable to the activity of the corresponding methoxy or benzamide derivatives reported in our previous studies.¹⁰

To obtain molecular insight into the ligand-binding site interactions, the X-ray crystal structure of **15g** bound to PLpro was determined. Interestingly, the binding mode and key molecular interactions of inhibitor **15g** are quite different than predicted and are different from the active-site interactions with the benzamide-derived inhibitors we previously reported. As shown in Figure 2, the inhibitor binds to a loop adjacent to the active site via a series of interactions including a hydrogen-bond formed between the carboxamide NH of the inhibitor and the backbone carbonyl of Tyr-269, with **15g** wrapped around the β-turn. The **15g** bound PLpro crystal structure also confirms the presence of a few structural water molecules conserved between the apo enzyme (PDB code

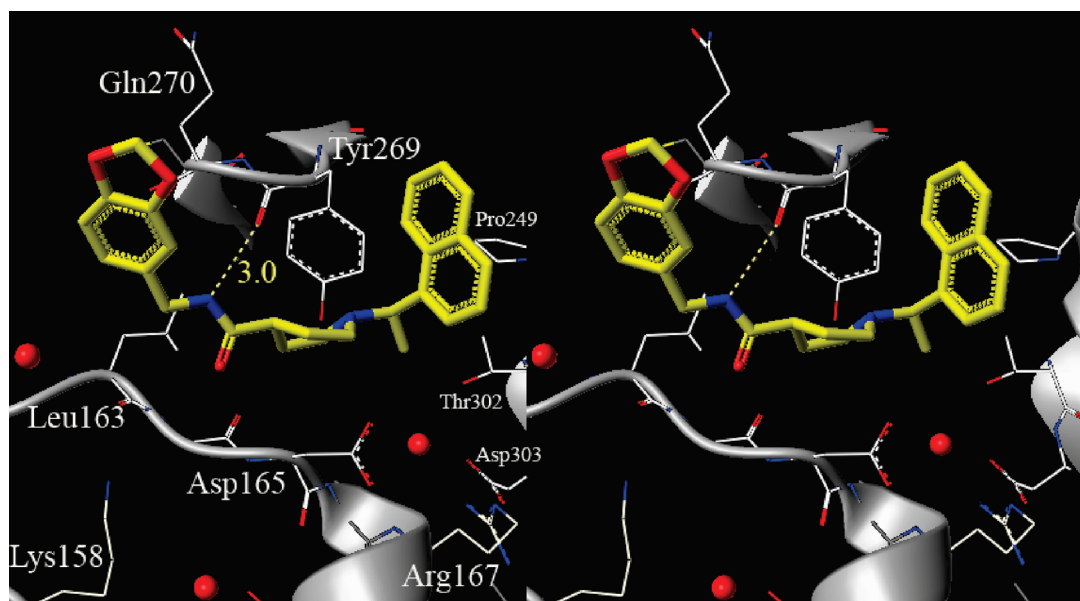


Figure 2. Stereorepresentation of **15g** bound to PLpro, including the conserved waters adjacent to the binding site that may influence the binding conformation, as described in the text.

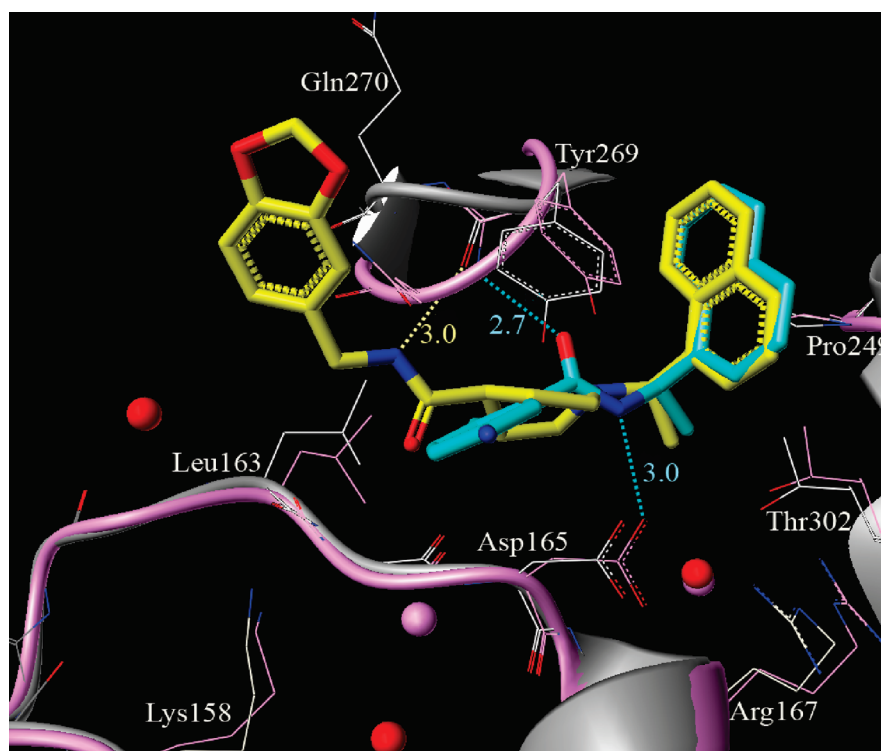


Figure 3. X-ray structure of inhibitor **15g**-bound (yellow) PLpro (gray) (PDB code 3MJ5) superimposed on the X-ray structure of inhibitor **2**-bound (cyan) PLpro (pink) (PDB code 3E9S).

2FE8) and inhibitor **2** bound PLpro (PDB code 3E9S). One of the conserved water molecules sits in the P5 pocket shown in Figure 2 as spheres between residues Asp-165, Asp-303, and Thr-302, preventing the inhibitor naphthyl rings from occupying this pocket. In the stereoimage of **15g**-bound PLpro we also show two other water molecules near residue Leu-163 and Lys-158 that may prevent the benzodioxolane ring from flipping down toward Lys-158.

Figure 3 superimposes **15g** and our previously developed inhibitor, **2**,¹⁰ and demonstrates that the binding mode differs

significantly between the two inhibitors. Interestingly, the turn region between Tyr-269 and Gln-270 also shows significant flexibility, particularly in the case of inhibitor **2** (PDB code 3E9S), where the peptide bond between Tyr-269 and Gln-270 flips by 180° to enable a hydrogen bond interaction between the backbone nitrogen of Tyr-269 and the carboxamide oxygen in inhibitor **2**. The carboxamide nitrogen makes a hydrogen bond with the side chain carboxylate of Asp-165. The carboxamide nitrogen of inhibitor **15g** (yellow) forms a hydrogen bond with the backbone carbonyl

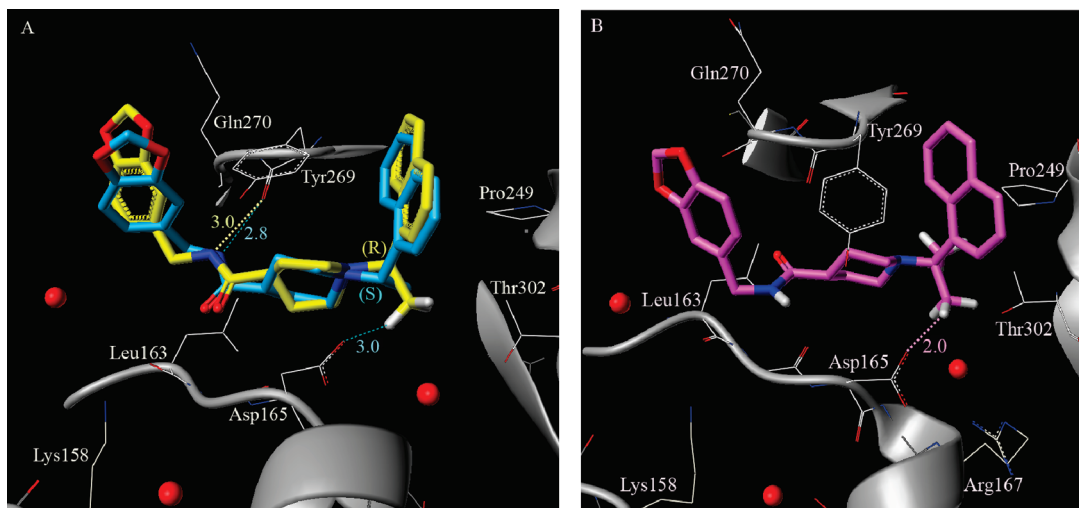


Figure 4. (A) Superposition of enantiomer **15h** (blue) with the crystal structure of **15g**-bound (yellow) PLpro. (B) Docked alignment of the *gem*-dimethyl substituted compound in the **15g**-ligand removed PLpro crystal structure. The bumping collision of one of the methyl groups of the *gem*-dimethyl (magenta) **15k** with the Asp-165 carboxylate is noted.

oxygen of Tyr-269 (protein shown in gray). The naphthyl rings of both inhibitors **2** and **15g** align in a similar fashion in the hydrophobic pocket formed by residues Tyr-269, Tyr-265, Pro-248, Pro-249, and Thr-302. The overlapping position of one conserved water molecule observed for both the inhibitor **2**-bound PLpro (oxygen atom shown as sphere in pink) crystal structure and inhibitor **15g**-bound PLpro (oxygen atom shown as sphere in red) crystal structure is shown as overlapping spheres.

Modeling Studies

To understand the SAR of the analogues of HTS hit compound **3**, we used computer modeling to explore the interactions of this series of inhibitors with PLpro. The activity of this series of compounds is independent of stereoisomerism in contrast to the series of compounds synthesized from the first HTS hit compound **1**.¹⁰ GOLD redocking of inhibitor **15g** into the PLpro crystal structure described above produces a heavy atom rmsd of 1.7 Å with the crystal structure conformation of **15g**, indicating that docking satisfactorily reproduces the experimental structure. When the inhibitors **15g**, **15h**, and **15k** are docked into the ligand removed **15g**-bound PLpro crystal structure (with residues Tyr-269 and Gln-270 flagged as flexible), the internal strain scores of the compounds correlate very well with their enzymatic activities. The conserved overlapping water molecules observed in both chains A and B of the **15g**-bound PLpro crystal structure were included for all docking studies.

To investigate the structural basis of the potency insensitivity to the (*R*)-Me (**15g**) versus (*S*)-Me (**15h**) configuration, we show the docked model of inhibitor **15h** superimposed on the crystal structure of **15g**-bound PLpro in Figure 4A. From this model, we observe an inversion of the piperidine ring between the (*R*)-Me and (*S*)-Me binding modes that allows the naphthyl rings of both isomers to be accommodated in the active site in very similar orientations. The flexible piperidine ring also acts as a spacer group that enables the carboxamide NH of both **15h** and **15g** to hydrogen-bond with the backbone carbonyl oxygen of Tyr-269 in a similar fashion, thereby retaining the potency of both enantiomers. However, the *gem*-dimethyl substitution in **15k** decreases the freedom around the carbon atom and locks the compound in a conformation where

one of the methyl groups exhibits a bumping collision with the side chain of Asp-165. One of the methyl groups in **15k** shifts almost 1.2 Å toward residue Asp-165 when compared to the single methyl substitution (*R*)-Me in **15g**, as can be seen in Figure 4B. It is important to note that the side chain of this Asp-165 is locked in its position by a hydrogen bond with the backbone NH of Arg-167. Hence, the *gem*-dimethyl substitution is not favorably accommodated in the active site because in order to fit the hydrophobic methyl group near the hydrophilic residue, the aspartic acid side chain would have to move out, thereby breaking structural hydrogen bonding with Arg-167.

This hypothesis is further validated by the GoldScore scoring function of GOLD, version 4.1, during the docking study. Compound **15k** is heavily penalized because of an unfavorable internal energy term (−12 compared to about −6 for both **15g** and **15h**) which is a sum of the internal torsional strain and internal van der Waals energy terms of the ligand. Docking with flexible residues also suggests that the Gln-270 side chain may adopt conformations that might enable hydrogen bonding interactions with one of the 1,3 benzodioxolane oxygens in **15g** and **15h** (within 3 Å). However, all docked conformations generated for **15k** show a loss of this hydrogen bonding interaction. The closest benzodioxolane oxygen of **15k** is at least 4.8 Å away from the side chain of Gln-270 (not shown). Figure 4B highlights the potential bumping collision of one of the methyl groups of **15k** with Asp-165, demonstrating that two methyl groups cannot be accommodated favorably at this position.

In our previous study, we discussed the SAR of the analogues of our first HTS hit **1** and the evolution of inhibitor **2** in great detail.¹⁰ In distinct contrast to the present work, that series of compounds is extremely sensitive to the enantiomeric form of the compound. From docking studies we concluded that the (*R*)-Me form was active whereas the (*S*)-Me was inactive because the (*S*)-Me conformation pushed the carboxamide group of the inhibitor away from the backbone NH of Tyr-269, inhibiting hydrogen bond formation with the loop residue.

Conclusion

We have designed, synthesized, and evaluated a novel series of SARS-CoV PLpro inhibitors. Initial lead structure **3**

($IC_{50} = 59.2 \mu M$) was discovered via high-throughput screening of a library of diverse compounds. Our preliminary structure–activity studies and systematic modification guided by X-ray crystal structure of **2**-bound PLpro and subsequent molecular modeling resulted in a potent inhibitor **15g** with enzyme inhibitory IC_{50} value of 320 nM and antiviral EC_{50} value of $9.1 \mu M$ in SARS-CoV-infected Vero E6 cells. Interestingly, the corresponding (*S*)-isomer **15h** is only slightly less potent ($IC_{50} = 560$ nM) in PLpro inhibitory assays but equipotent in antiviral assays. The corresponding *gem*-dimethyl derivative **15k** is significantly less potent. A protein–ligand X-ray structure of **15g**-bound PLpro was determined to 2.6 Å resolution. This structure provided critical molecular insight into the ligand binding site interactions. It appears that the key active site interactions are quite different from the earlier series of inhibitors. Further design of improved reversible SARS-CoV PLpro inhibitors is currently underway in our laboratories.

Experimental Section

Chemistry. 1H NMR and ^{13}C NMR spectra were recorded on Varian Oxford 300 and Bruker Avance 400 spectrometers. Optical rotations were recorded on a Perkin-Elmer 341 polarimeter. Anhydrous solvent was obtained as follows: CH_2Cl_2 by distillation from CaH_2 , THF by distillation from Na and benzophenone. All other solvents were reagent grade. Column chromatography was performed with Whatman 240–400 mesh silica gel under a low pressure of 3–5 psi. TLC was carried out with E. Merck silica gel 60-F-254 plates. Purity of all test compounds was determined by HRMS and HPLC analysis in the different solvent systems. All test compounds showed $\geq 95\%$ purity.

1-(*tert*-Butoxycarbonyl)-4-[(3-methoxybenzylamino)carbonyl]piperidine (6b). To a solution of 1-(*tert*-butoxycarbonyl)piperidine-4-carboxylic acid (344 mg, 1.5 mmol) in dry CH_2Cl_2 (5 mL), 1-ethyl-3-(3-dimethylaminopropyl)carbodiimide hydrochloride (EDC·HCl) (287 mg, 1.5 mmol), 1-hydroxybenzotriazole hydrate (HOBt·H₂O) (203 mg, 1.5 mmol), *N*-methylmorpholine (NMM) (0.16 mL, 1.5 mmol), and 3-methoxybenzylamine (0.13 mL, 1 mmol) were added successively at 23 °C under argon atmosphere, and the resulting reaction mixture was stirred for 5 h at the same temperature. The reaction mixture was quenched with aqueous NaOH solution and extracted with CH_2Cl_2 . The organic layers were dried over anhydrous Na_2SO_4 , filtered, and concentrated under reduced pressure. The residue was purified by silica gel column chromatography (40% EtOAc/hexanes) to furnish **6b** (327 mg, 94%) as a viscous liquid. 1H NMR (400 MHz, $CDCl_3$): δ 7.24 (t, $J = 7.6$ Hz, 1H), 6.76–6.86 (m, 3H), 5.78 (br, 1H), 4.41 (d, $J = 5.6$ Hz, 2H), 4.12 (br, 2H), 3.79 (s, 3H), 2.73 (br t, $J = 11.2$ Hz, 2H), 2.25 (tt, $J = 4.0$ and 11.6 Hz, 1H), 1.82 (br d, $J = 12.0$ Hz, 2H), 1.65 (ddd, $J = 4.1$, 12.2, and 24.8 Hz, 2H), 1.45 (s, 9H). ^{13}C NMR (100 MHz, $CDCl_3$): δ 174.1, 159.9, 154.6, 139.7, 129.8, 119.9, 113.4, 112.9, 79.6, 55.2, 43.5, 43.4, 28.6, 28.4.

1-(*tert*-Butoxycarbonyl)-4-[(2-methoxybenzylamino)carbonyl]piperidine (6a). The title compound **6a** was obtained as described for compound 1-(*tert*-butoxycarbonyl)-4-[(3-methoxybenzylamino)carbonyl]piperidine in 92% yield (viscous liquid). 1H NMR (400 MHz, $CDCl_3$): δ 7.22 (br t, $J = 7.2$ Hz, 2H), 6.83–6.92 (m, 2H), 6.09 (br, 1H), 4.41 (d, $J = 5.8$ Hz, 2H), 4.09 (br, 2H), 3.83 (s, 3H), 2.70 (br t, $J = 11.1$ Hz, 2H), 2.20 (tt, $J = 3.7$ and 11.6 Hz, 1H), 1.77 (br d, $J = 12.0$ Hz, 2H), 1.59 (ddd, $J = 4.4$, 12.0, and 24.8 Hz, 2H), 1.43 (s, 9H). ^{13}C NMR (100 MHz, $CDCl_3$): δ 173.9, 157.5, 154.6, 129.6, 128.8, 126.1, 120.6, 110.3, 79.5, 55.3, 43.2, 39.2, 28.5, 28.3.

1-[(1-Naphthyl)methyl]-4-[(3-methoxybenzylamino)carbonyl]piperidine (7b). To a solution of 1-(*tert*-butoxycarbonyl)-4-[(3-methoxybenzylamino)carbonyl]piperidine (100 mg, 0.287

mmol) in CH_2Cl_2 (3 mL), trifluoroacetic acid (0.15 mL) was added at 0 °C. The resulting mixture was stirred for 6 h at 23 °C. The reaction mixture was diluted with CH_2Cl_2 and basified by slow addition of saturated $NaHCO_3$ solution. The layers were separated and the aqueous layer was extracted several times with ethyl acetate. The combined organic layers were dried over anhydrous Na_2SO_4 . The solvent was removed under reduced pressure to furnish the amine. To the crude amine in dry CH_2Cl_2 (5 mL), 1-naphthaldehyde (77 μL , 0.57 mmol), $Na(OAc)_3BH$ (121 mg, 0.57 mmol), and AcOH (33 μL , 0.57 mmol) were added successively at 23 °C, and the resulting mixture was stirred for 12 h at 23 °C. The reaction mixture was basified with 2 N NaOH and diluted with CH_2Cl_2 and H_2O . The organic layer was separated and the aqueous layer extracted with CH_2Cl_2 . The combined organic layers were dried over anhydrous Na_2SO_4 . Solvent was removed under reduced pressure and the resulting residue was purified by column chromatography over silica gel (2% MeOH/ CH_2Cl_2) to provide 1-[(1-naphthyl)methyl]-4-[(3-methoxybenzylamino)carbonyl]piperidine as a viscous liquid (79 mg, 71%). 1H NMR (400 MHz, $CDCl_3$): δ 8.28–8.33 (m, 1H), 7.82–7.88 (m, 1H), 7.77 (dd, $J = 2.2$ and 7.1 Hz, 1H), 7.44–7.53 (m, 2H), 7.36–7.43 (m, 2H), 7.23 (t, $J = 7.8$ Hz, 1H), 6.77–6.86 (m, 3H), 5.79 (br, 1H), 4.40 (d, $J = 5.7$ Hz, 2H), 3.88 (s, 2H), 3.78 (s, 3H), 2.94–3.04 (m, 2H), 2.15 (tt, $J = 4.2$ and 11.4 Hz, 1H), 2.06 (dt, $J = 2.7$ and 11.3 Hz, 2H), 1.72–1.88 (m, 4H). ^{13}C NMR (100 MHz, $CDCl_3$): δ 174.9, 159.8, 139.9, 134.3, 133.8, 132.5, 129.7, 128.3, 127.8, 127.2, 125.7, 125.6, 125.0, 124.8, 119.9, 113.3, 112.9, 61.3, 55.2, 53.3, 43.6, 43.3, 29.1. IR (neat): 3290, 2922, 1644, 1598, 1263 cm^{-1} . MS (ESI): m/z 389 $[M + H]^+$.

1-[(1-Naphthyl)methyl]-4-[(2-methoxybenzylamino)carbonyl]piperidine (7a). The title compound **7a** was obtained as described for compound **7b** in 70% yield (viscous liquid). 1H NMR (400 MHz, $CDCl_3$): δ 8.30 (d, $J = 7.9$ Hz, 1H), 7.84 (d, $J = 7.1$ Hz, 1H), 7.77 (d, $J = 7.1$ Hz, 1H), 7.44–7.53 (m, 2H), 7.37–7.43 (m, 2H), 7.21–7.30 (m, 2H), 6.83–6.94 (m, 2H), 5.98 (br s, 1H), 4.43 (d, $J = 5.6$ Hz, 2H), 3.87 (s, 2H), 3.84 (s, 3H), 2.98 (d, $J = 11.2$ Hz, 2H), 2.01–2.20 (m, 3H), 1.68–1.84 (m, 4H). ^{13}C NMR (100 MHz, $CDCl_3$): δ 174.6, 157.5, 134.3, 133.8, 132.5, 129.8, 128.8, 128.3, 127.8, 127.2, 126.3, 125.7, 125.6, 125.1, 124.8, 120.7, 110.3, 61.3, 55.3, 53.4, 43.6, 39.3, 29.0. IR (neat): 3305, 1643, 1600, 1242 cm^{-1} . MS (ESI): m/z 389 $[M + H]^+$.

1-[(*R*)-1-(1-Naphthyl)ethyl]-4,4-bis(methoxycarbonyl)-1,4-dihydropyridine (12a). A solution of malonate **10** (1.8 g, 5.92 mmol) in 10% hydrochloric acid solution (35 mL) and THF (35 mL) was stirred for 18 h at 23 °C. The solution was neutralized with powdered sodium hydrogen carbonate, and then 1-(*R*)-naphthylmethylamine **11a** (1.0 g, 5.84 mmol) in THF (5 mL) was added. After the mixture was stirred for 16 h at 23 °C, the aqueous layer was extracted with EtOAc and dried over Na_2SO_4 . Removal of the solvent afforded the residue, which was purified by silica gel column chromatography to furnish compound **12a** (1.1 g, 54%) as a colorless oil. $R_f = 0.74$ (hexane/EtOAc = 1:1). $[\alpha]_D^{20} -58$ (c 1, $CHCl_3$). 1H NMR (300 MHz, $CDCl_3$): δ 7.90 (d, 1H, $J = 7.8$ Hz), 7.84 (d, 1H, $J = 7.8$ Hz), 7.80–7.75 (m, 1H), 7.54–7.40 (m, 4H), 6.21 (d, 2H, $J = 8.3$ Hz), 5.16 (q, 1H, $J = 6.6$ Hz), 4.77 (d, 2H, $J = 8.3$ Hz), 3.69 (s, 6H), 1.67 (d, 3H, $J = 6.6$ Hz). ^{13}C NMR (75 MHz, $CDCl_3$): δ 171.4, 136.2, 133.7, 130.8, 129.2, 128.7, 128.4, 126.3, 125.5, 124.9, 123.7, 122.8, 95.3, 56.8, 54.0, 52.4, 19.4. IR (neat): 2951, 1736, 1249, 1069 cm^{-1} . MS (EI): m/z 352 $[M + H]^+$. HRMS (EI), calcd for $C_{21}H_{22}NO_4$ 352.1549, found 352.1553.

1-[(*R*)-1-(2-Naphthyl)ethyl]-4,4-bis(methoxycarbonyl)-1,4-dihydropyridine (12b). The title compound was obtained as described in compound **12a** in 58% yield (colorless oil). $R_f = 0.79$ (hexane/EtOAc = 1:1). $[\alpha]_D^{20} +32$ (c 1, $CHCl_3$). 1H NMR (300 MHz, $CDCl_3$): δ 7.84–7.78 (m, 3H), 7.66 (s, 1H), 7.49–7.43 (m, 2H), 7.33 (dd, 1H, $J = 1.5$ and 8.7 Hz), 6.21 (d, 2H, $J = 8.3$ Hz), 4.78 (d, 2H, $J = 8.3$ Hz), 4.59 (q, 1H, $J = 6.9$ Hz), 3.72 (s, 6H), 1.64 (d, 3H, $J = 6.9$ Hz). ^{13}C NMR (75 MHz,

CDCl₃): δ 171.6, 139.2, 133.1, 132.6, 129.6, 128.4, 127.9, 127.7, 127.5, 126.2, 125.9, 124.8, 95.3, 60.4, 54.1, 52.6, 19.5. IR (neat): 2952, 1732, 1253, 1069 cm⁻¹. MS (EI): m/z 292 [M - CO₂Me]⁺. HRMS (EI), calcd for C₁₉H₁₈NO₂ 292.1337, found [M - CO₂Me]⁺ 292.1345.

1-[(S)-1-(2-Naphthyl)ethyl]-4,4-bis(methoxycarbonyl)-1,4-dihydropyridine (12c). The title compound was obtained as described in compound **12a** in 54% yield (colorless oil). R_f = 0.73 (hexane/EtOAc = 1:1). [α]_D²⁰ -32 (*c* 1, CHCl₃). MS (EI): m/z 351 [M]⁺. HRMS (EI), calcd for C₂₁H₂₁NO₄ 351.1471, found [M]⁺ 351.1477.

1-[(S)-1-(1-Naphthyl)ethyl]-4,4-bis(methoxycarbonyl)-1,4-dihydropyridine (12d). The title compound was obtained as described in compound **12a** in 42% yield (colorless oil). R_f = 0.77 (hexane/EtOAc = 1:1). [α]_D²⁰ +57 (*c* 1, CHCl₃). MS (ESI): m/z 374 [M + Na]⁺. HRMS (ESI), calcd for C₂₁H₂₁NO₄Na 374.1368, found 374.1371.

1-(1-Naphthylmethyl)-4,4-bis(methoxycarbonyl)-1,4-dihydropyridine (12e). The title compound was obtained as described in compound **12a** in 39% yield (colorless oil). R_f = 0.82 (hexane/EtOAc = 1:1). ¹H NMR (300 MHz, CDCl₃): δ 7.86–7.80 (m, 2H), 7.77 (d, 1H, *J* = 8.7 Hz), 7.54–7.48 (m, 2H), 7.42 (t, 1H, *J* = 8.3 Hz), 7.30 (d, 1H, *J* = 6.9 Hz), 6.15 (d, 2H, *J* = 8.3 Hz), 4.82 (d, 2H, *J* = 8.3 Hz), 4.74 (s, 2H), 3.73 (s, 6H). ¹³C NMR (75 MHz, CDCl₃): δ 171.6, 133.5, 132.6, 131.1, 130.7, 128.7, 128.2, 126.4, 125.8, 125.4, 125.1, 122.5, 95.3, 54.5, 53.7, 52.7. IR (neat): 2951, 1735, 1253, 1067 cm⁻¹. MS (EI): m/z 278 [M - CO₂Me]⁺. HRMS (EI), calcd for C₁₈H₁₆NO₂ 278.1181, found 278.1185.

1-(2-Naphthylmethyl)-4,4-bis(methoxycarbonyl)-1,4-dihydropyridine (12f). The title compound was obtained as described in compound **12a** in 62% yield (colorless oil). R_f = 0.80 (hexane/EtOAc = 1:1). ¹H NMR (300 MHz, CDCl₃): δ 7.80–7.77 (m, 3H), 7.60 (s, 1H), 7.48–7.41 (m, 2H), 7.28 (d, 1H, *J* = 1.8 Hz), 6.16 (d, 2H, *J* = 8.0 Hz), 4.81 (d, 2H, *J* = 8.0 Hz), 4.41 (s, 2H), 3.73 (s, 6H). ¹³C NMR (75 MHz, CDCl₃): δ 171.5, 134.9, 133.1, 132.6, 131.2, 128.5, 127.7, 127.5, 126.2, 125.9, 125.8, 124.8, 95.3, 56.9, 53.6, 52.6. IR (neat): 2950, 1731, 1253, 1066 cm⁻¹. MS (EI): m/z 278 [M - CO₂Me]⁺. HRMS (EI), calcd for C₁₈H₁₆NO₂ 278.1181, found 278.1184.

1-[1-Methyl-1-(1-naphthyl)ethyl]-4,4-bis(methoxycarbonyl)-1,4-dihydropyridine (12g). The title compound was obtained as described in compound **12a** in 41% yield (colorless oil). R_f = 0.77 (hexane/EtOAc = 1:1). ¹H NMR (300 MHz, CDCl₃): δ 8.20–8.16 (m, 1H), 7.89 (d, 1H, *J* = 7.8 Hz), 7.84–7.80 (m, 1H), 7.77 (d, 1H, *J* = 7.8 Hz), 7.52–7.36 (m, 4H), 6.27 (d, 2H, *J* = 8.1 Hz), 4.77 (d, 2H, *J* = 8.1 Hz), 3.69 (s, 6H), 1.77 (s, 6H). ¹³C NMR (75 MHz, CDCl₃): δ 171.6, 140.1, 134.7, 130.5, 129.1, 129.0, 127.7, 126.1, 126.0, 125.3, 124.7, 124.0, 96.0, 61.9, 53.8, 52.5, 28.7. IR (neat): 2951, 1736, 1252, 1062 cm⁻¹. MS (ESI): m/z 388 [M + Na]⁺. HRMS (ESI), calcd for C₂₂H₂₃NO₄Na 388.1525, found 388.1529.

1-[(R)-1-(1-Naphthyl)ethyl]-4,4-bis(methoxycarbonyl)piperidine (13a). To a stirred solution of dihydropyridine **12a** (1.1 g, 3.1 mmol) in EtOAc (75 mL) was added platinum(IV) oxide (100 mg), and the mixture was allowed to stir for 2 h at 23 °C under H₂ atmosphere. The mixture was filtered through Celite pad, and the filtrate was concentrated under reduced pressure. The residue was purified by silica gel column chromatography to furnish compound **13a** (942 mg, 88%) as a colorless oil. R_f = 0.7 (hexane/EtOAc = 1:1). [α]_D²⁰ +9 (*c* 1, CHCl₃). ¹H NMR (300 MHz, CDCl₃): δ 8.44–8.41 (m, 1H), 7.85–7.81 (m, 1H), 7.73 (d, 1H, *J* = 8.1 Hz), 7.56 (d, 1H, *J* = 6.9 Hz), 7.50–7.39 (m, 3H), 4.03–3.73 (q, 1H, *J* = 6.3 Hz), 3.72 (s, 6H), 2.58–2.56 (m, 2H), 2.47–2.40 (m, 2H), 2.20–2.04 (m, 4H), 1.44 (d, 3H, *J* = 6.3 Hz). ¹³C NMR (75 MHz, CDCl₃): δ 171.8, 140.7, 134.0, 131.5, 128.6, 127.3, 125.4, 125.3, 125.2, 124.5, 124.1, 61.7, 53.3, 52.4, 47.9, 31.2, 18.7. IR (neat): 2952, 1734, 1251 cm⁻¹. MS (ESI): m/z 356 [M + H]⁺. HRMS (ESI), calcd for C₂₁H₂₆NO₄ 356.1862, found 356.1866.

1-[(R)-1-(2-Naphthyl)ethyl]-4,4-bis(methoxycarbonyl)piperidine (13b). The title compound was obtained as described in

compound **13a** in 74% yield (colorless oil). R_f = 0.48 (hexane/EtOAc = 1:1). [α]_D²⁰ +23 (*c* 1, CHCl₃). ¹H NMR (400 MHz, CDCl₃): δ 7.83–7.80 (m, 3H), 7.72 (s, 1H), 7.53 (dd, 1H, *J* = 1.3 and 8.7 Hz), 7.49–7.42 (m, 2H), 3.73 (s, 6H), 3.49 (q, 1H, *J* = 6.7 Hz), 2.57–2.55 (bm, 2H), 2.47–2.42 (m, 2H), 2.24–2.13 (m, 4H), 1.42 (d, 3H, *J* = 6.7 Hz). ¹³C NMR (100 MHz, CDCl₃): δ 171.7, 142.1, 133.3, 132.7, 128.0, 127.7, 127.5, 125.8, 125.8, 125.4, 64.8, 53.2, 52.5, 47.9, 31.1, 19.6. IR (neat): 2951, 1731, 1250, 1073 cm⁻¹. MS (EI): m/z 355 [M]⁺. HRMS (EI), calcd for C₂₁H₂₅NO₄ 355.1784, found 355.1781.

1-[(S)-1-(2-Naphthyl)ethyl]-4,4-bis(methoxycarbonyl)piperidine (13c). The title compound was obtained as described in compound **13a** in 67% yield (colorless oil). R_f = 0.48 (hexane/EtOAc = 1:1). [α]_D²⁰ -24 (*c* 1, CHCl₃). MS (EI): m/z 355 [M]⁺. HRMS (EI), calcd for C₂₁H₂₅NO₄ 355.1784, found 355.1786.

1-[(S)-1-(1-Naphthyl)ethyl]-4,4-bis(methoxycarbonyl)piperidine (13d). The title compound was obtained as described in compound **13a** in 87% yield (colorless oil). R_f = 0.7 (hexane/EtOAc = 1:1). [α]_D²⁰ -9 (*c* 1, CHCl₃). MS (ESI): m/z 356 [M + H]⁺. HRMS (ESI), calcd for C₂₁H₂₆NO₄ 356.1862, found 356.1865.

1-(1-Naphthylmethyl)-4,4-bis(methoxycarbonyl)piperidine (13e). The title compound was obtained as described in compound **13a** in 60% yield (colorless oil). R_f = 0.70 (hexane/EtOAc = 1:1). ¹H NMR (300 MHz, CDCl₃): δ 8.29–8.26 (m, 1H), 7.84–7.81 (m, 1H), 7.77–7.73 (m, 1H), 7.52–7.43 (m, 2H), 7.38–7.36 (m, 2H), 3.84 (s, 2H), 3.72 (s, 6H), 2.48 (t, 4H, *J* = 5.4 Hz), 2.13 (t, 4H, *J* = 5.4 Hz). ¹³C NMR (75 MHz, CDCl₃): δ 171.7, 134.1, 133.8, 132.5, 128.3, 127.9, 127.2, 125.6, 125.5, 125.0, 124.8, 61.2, 53.3, 52.5, 50.6, 31.0. IR (neat): 2950, 1732, 1254, 1072 cm⁻¹. MS (EI): m/z 341 [M]⁺. HRMS (EI), calcd for C₂₀H₂₃NO₄ 341.1627, found 341.1630.

1-(2-Naphthylmethyl)-4,4-bis(methoxycarbonyl)piperidine (13f). The title compound was obtained as described in compound **13a** in 94% yield (colorless oil). R_f = 0.48 (hexane/EtOAc = 1:1). ¹H NMR (400 MHz, CDCl₃): δ 7.83–7.78 (m, 3H), 7.72 (s, 1H), 7.50–7.42 (m, 3H), 3.74 (s, 6H), 3.61 (s, 2H), 2.48 (bm, 4H), 2.19 (t, 4H, *J* = 5.5 Hz). ¹³C NMR (100 MHz, CDCl₃): δ 171.7, 135.9, 133.2, 132.7, 127.8, 127.6, 127.5, 127.2, 125.9, 125.5, 63.2, 53.2, 52.5, 50.5, 30.9. IR (neat): 2950, 1732, 1254, 1073 cm⁻¹. MS (EI): m/z 341 [M]⁺. HRMS (EI), calcd for C₂₀H₂₃NO₄ 341.1627, found [M]⁺ 341.1626.

1-[1-Methyl-1-(1-naphthyl)ethyl]-4,4-bis(methoxycarbonyl)piperidine (13g). The title compound **13g** was obtained as described in compound **13a** in 93% yield (colorless oil). R_f = 0.29 (hexane/EtOAc = 9:1). ¹H NMR (400 MHz, CDCl₃): δ 9.59 (d, 1H, *J* = 7.9 Hz), 7.84 (dd, 1H, *J* = 2.2 and 7.0 Hz), 7.74 (d, 1H, *J* = 8.0 Hz), 7.52–7.44 (m, 3H), 7.37 (t, 1H, *J* = 7.7 Hz), 3.74 (s, 6H), 2.63 (bm, 4H), 2.14 (bm, 4H), 1.59 (s, 6H). ¹³C NMR (100 MHz, CDCl₃): δ 171.8, 143.7, 134.9, 132.0, 128.6, 128.2, 128.0, 125.1, 124.7, 124.4, 123.6, 62.2, 53.6, 52.4, 43.4, 31.8, 23.6. IR (neat): 2973, 1735, 1251, 1124, 780 cm⁻¹. MS (ESI): m/z 370 [M + H]⁺. HRMS (ESI), calcd for C₂₂H₂₈NO₄ 370.2018, found 370.2013.

1-[(R)-1-(1-Naphthyl)ethyl]-4-methoxycarbonylpiperidine (14a). To a stirred solution of dimethyl malonate **13a** (917 mg, 2.58 mmol) in DMF (25 mL) was added sodium cyanide (190 mg, 3.88 mmol) at 23 °C, and the mixture was allowed to stir for 16 h at reflux temperature. The mixture was diluted with EtOAc and washed with water. The organic layer was dried over Na₂SO₄, filtered, and concentrated. The residue was purified by silica gel column chromatography to furnish compound **14a** (704 mg, 92%) as a colorless oil. R_f = 0.56 (CH₂Cl₂/MeOH = 9:1). [α]_D²⁰ +2 (*c* 1, CHCl₃). ¹H NMR (400 MHz, CDCl₃): δ 8.48 (dd, 1H, *J* = 1.2 and 7.6 Hz), 7.87 (d, 1H, *J* = 7.1 Hz), 7.76 (d, 1H, *J* = 8.1 Hz), 7.60 (d, 1H, *J* = 7.1 Hz), 7.53–7.43 (m, 3H), 4.12 (q, 1H, *J* = 6.7 Hz), 3.68 (s, 3H), 3.17–3.15 (m, 1H), 2.87–2.84 (m, 1H), 2.35–2.27 (m, 1H), 2.10 (ddd, 2H, *J* = 2.6, 11.2, and 19.8 Hz), 1.97–1.92 (m, 1H), 1.83–1.71 (m, 3H), 1.49 (d, 3H, *J* = 6.7 Hz). ¹³C NMR (100 MHz, CDCl₃): δ 175.8, 140.8, 134.0, 131.6, 128.6, 127.2, 125.4, 125.3, 125.3, 124.5, 124.2, 61.6, 51.5, 49.1, 41.3, 28.7,

28.6, 18.6. IR (neat): 2950, 1732, 1169, 780 cm^{-1} . MS (EI): m/z 297 $[\text{M}]^+$. HRMS (EI), calcd for $\text{C}_{19}\text{H}_{23}\text{NO}_2$ 297.1729, found 297.1730.

1-[(R)-1-(2-Naphthyl)ethyl]-4-methoxycarbonylpiperidine (14b). The title compound was obtained as described in compound **14a** in 78% yield (colorless oil). $R_f = 0.43$ ($\text{CH}_2\text{Cl}_2/\text{MeOH} = 9:1$). $[\alpha]_{\text{D}}^{20} +16$ (c 1, CHCl_3). ^1H NMR (400 MHz, CDCl_3): δ 7.84–7.80 (m, 3H), 7.72 (s, 1H), 7.53 (dd, 1H, $J = 1.1$ and 8.4 Hz), 7.50–7.43 (m, 2H), 3.67 (s, 3H), 3.57 (q, 1H, $J = 6.8$ Hz), 3.08–3.06 (m, 1H), 2.86–2.83 (m, 1H), 2.29–2.22 (m, 1H), 2.09–1.91 (m, 3H), 1.87–1.71 (m, 3H), 1.45 (d, 3H, $J = 6.8$ Hz). ^{13}C NMR (100 MHz, CDCl_3): δ 175.7, 141.7, 133.3, 132.7, 127.8, 127.7, 127.5, 126.0, 125.9, 125.8, 125.4, 64.7, 51.5, 50.5, 49.6, 41.2, 28.5, 19.3. IR (neat): 2949, 1732, 1258, 1172 cm^{-1} . MS (EI): m/z 297 $[\text{M}]^+$. HRMS (EI), calcd for $\text{C}_{19}\text{H}_{23}\text{NO}_2$ 297.1729, found $[\text{M}]^+$ 297.1732.

1-[(S)-1-(2-Naphthyl)ethyl]-4-methoxycarbonylpiperidine (14c). The title compound was obtained as described in compound **14a** in 90% yield (colorless oil). $R_f = 0.47$ ($\text{CH}_2\text{Cl}_2/\text{MeOH} = 9:1$). $[\alpha]_{\text{D}}^{20} -15$ (c 1, CHCl_3). MS (EI): m/z 297 $[\text{M}]^+$. HRMS (EI), calcd for $\text{C}_{19}\text{H}_{23}\text{NO}_2$ 297.1729, found 297.1731.

1-[(S)-1-(1-Naphthyl)ethyl]-4-methoxycarbonylpiperidine (14d). The title compound was obtained as described in compound **14a** in 76% yield (colorless oil). $R_f = 0.57$ ($\text{CH}_2\text{Cl}_2/\text{MeOH} = 9:1$). $[\alpha]_{\text{D}}^{20} -2$ (c 1, CHCl_3). MS (EI): m/z 297 $[\text{M}]^+$. HRMS (EI), calcd for $\text{C}_{19}\text{H}_{23}\text{NO}_2$ 297.1729, found 297.1729.

1-(1-Naphthylmethyl)-4-methoxycarbonylpiperidine (14e). The title compound was obtained as described in compound **14a** in 38% yield (colorless oil). $R_f = 0.53$ ($\text{CH}_2\text{Cl}_2/\text{MeOH} = 9:1$). ^1H NMR (400 MHz, CDCl_3): δ 8.31 (d, 1H, $J = 7.8$ Hz), 7.86 (dd, 1H, $J = 1.6$ and 7.1 Hz), 7.78 (d, 1H, $J = 7.1$ Hz), 7.53–7.47 (m, 2H), 7.44–7.39 (m, 2H), 3.89 (s, 2H), 3.68 (s, 3H), 2.94–2.88 (m, 2H), 2.37–2.30 (m, 1H), 2.12 (dt, 2H, $J = 1.6$ and 11.2 Hz), 1.90–1.86 (m, 2H), 1.81–1.72 (m, 2H). ^{13}C NMR (100 MHz, CDCl_3): δ 175.7, 134.2, 133.7, 132.5, 128.3, 127.8, 127.2, 125.6, 125.5, 125.0, 124.7, 61.3, 53.1, 51.5, 41.1, 28.3. IR (neat): 2949, 1736, 1167, 788 cm^{-1} . MS (EI): m/z 283 $[\text{M}]^+$. HRMS (EI), calcd for $\text{C}_{18}\text{H}_{21}\text{NO}_2$ 283.1572, found 283.1569.

1-(2-Naphthylmethyl)-4-methoxycarbonylpiperidine (14f). The title compound was obtained as described in compound **14a** in 47% yield (colorless oil). $R_f = 0.44$ ($\text{CH}_2\text{Cl}_2/\text{MeOH} = 9:1$). ^1H NMR (400 MHz, CDCl_3): δ 7.84–7.80 (m, 3H), 7.73 (s, 1H), 7.51–7.43 (m, 3H), 3.68 (s, 3H), 3.65 (s, 2H), 2.93–2.88 (m, 2H), 2.36–2.28 (m, 1H), 2.08 (dt, 2H, $J = 2.2$ and 11.4 Hz), 1.94–1.75 (m, 4H). ^{13}C NMR (100 MHz, CDCl_3): δ 175.6, 135.9, 133.2, 132.7, 127.8, 127.6, 127.6, 127.5, 127.3, 125.9, 125.5, 63.3, 52.9, 51.6, 41.0, 28.2. IR (neat): 2948, 1736, 1167 cm^{-1} . MS (ESI): m/z 284 $[\text{M} + \text{H}]^+$. HRMS (ESI), calcd for $\text{C}_{18}\text{H}_{22}\text{NO}_2$ 284.1651, found 284.1652.

1-[1-Methyl-1-(1-naphthyl)ethyl]-4-methoxycarbonylpiperidine (14g). The title compound was obtained as described in compound **14a** in 87% yield (colorless oil). $R_f = 0.43$ (hexane/ $\text{EtOAc} = 9:1$). ^1H NMR (400 MHz, CDCl_3): δ 9.63–9.60 (m, 1H), 7.87–7.84 (m, 1H), 7.76 (d, 1H, $J = 8.0$ Hz), 7.51–7.46 (m, 3H), 7.39 (t, 1H, $J = 7.8$ Hz), 3.69 (s, 3H), 2.96 (bs, 2H), 2.34–2.28 (m, 3H), 1.84–1.75 (bm, 4H), 1.61 (s, 6H). ^{13}C NMR (100 MHz, CDCl_3): δ 175.9, 144.1, 134.8, 132.0, 128.6, 128.4, 127.9, 125.1, 124.7, 124.4, 123.5, 62.3, 51.5, 45.9, 41.9, 29.2, 22.7. IR (neat): 2950, 1736, 1171, 780 cm^{-1} . MS (EI): m/z 311 $[\text{M}]^+$. HRMS (EI), calcd for $\text{C}_{20}\text{H}_{25}\text{NO}_2$ 311.1885, found 311.1891.

1-[(R)-1-(1-Naphthyl)ethyl]-4-(2-methoxybenzylamino)carbonylpiperidine (15a). To a stirred solution of ester **14a** (106 mg, 0.36 mmol) in THF/MeOH/ H_2O (3:1:1) (8 mL) was added $\text{LiOH} \cdot \text{H}_2\text{O}$ (22.4 mg, 0.53 mmol) at 0°C , and the mixture was allowed to stir for 16 h at 23°C . The mixture was concentrated, and to it was added a saturated NaHCO_3 solution. The mixture was extracted with Et_2O . The aqueous layer was adjusted to pH 2 with 10% HCl solution and extracted with EtOAc . The organic layers were dried over Na_2SO_4 , filtered, and concentrated to give the corresponding acid as a colorless oil. To a solution of acid (0.36 mmol),

N-(3-dimethylaminopropyl)-*N'*-ethylcarbodiimide hydrochloride (EDCI) (138.0 mg, 0.72 mmol) and 1-hydroxybenzotriazole hydrate (HOBT) (97.3 mg, 0.72 mmol) in dry $\text{CH}_2\text{Cl}_2/\text{DMF}$ (9:1) (8 mL) were added 2-methoxybenzylamine **5a** (52.7 μL , 0.40 mmol) and diisopropylethylamine (0.38 mL, 2.2 mmol) at 0°C under argon atmosphere. The mixture was allowed to stir for 15 h at 23°C . The reaction mixture was quenched with water and extracted with CH_2Cl_2 . The organic layers were dried over Na_2SO_4 , filtered, and concentrated under reduced pressure. The residue was purified by silica gel column chromatography to furnish compound **15a** (143 mg, 99%) as a white amorphous solid. $R_f = 0.42$ ($\text{CH}_2\text{Cl}_2/\text{MeOH} = 9:1$). $[\alpha]_{\text{D}}^{20} -2$ (c 1, CHCl_3). ^1H NMR (400 MHz, CDCl_3): δ 8.46 (d, 1H, $J = 7.8$ Hz), 7.86–7.84 (m, 1H), 7.74 (d, 1H, $J = 8.1$ Hz), 7.58 (d, 1H, $J = 7.0$ Hz), 7.51–7.41 (m, 3H), 7.23 (d, 1H, $J = 7.3$ Hz), 6.90 (t, 1H, $J = 7.3$ Hz), 6.85 (d, 1H, $J = 8.4$ Hz), 6.17 (bt, 1H, $J = 5.8$ Hz), 4.44 (d, 2H, $J = 5.8$ Hz), 4.10 (q, 1H, $J = 6.6$ Hz), 3.81 (s, 3H), 3.23–3.20 (m, 1H), 2.87–2.85 (m, 1H), 2.12–1.95 (m, 3H), 1.89–1.68 (m, 4H), 1.47 (d, 3H, $J = 6.6$ Hz). ^{13}C NMR (100 MHz, CDCl_3): δ 174.9, 157.5, 140.9, 134.1, 131.7, 129.6, 128.7, 128.7, 127.3, 126.5, 125.5, 125.4, 125.3, 124.5, 124.3, 120.7, 110.3, 61.7, 55.3, 52.0, 49.2, 43.7, 39.1, 29.3, 18.7. IR (neat): 3302, 2938, 1650, 1243, 753 cm^{-1} . MS (ESI): m/z 403 $[\text{M} + \text{H}]^+$. HRMS (ESI), calcd for $\text{C}_{26}\text{H}_{31}\text{N}_2\text{O}_2$ 403.2386, found 403.2388.

1-[(R)-1-(1-Naphthyl)ethyl]-4-(3-methoxybenzylamino)carbonylpiperidine (15b). The title compound was obtained as described in compound **15a** in 95% yield (white amorphous solid). $R_f = 0.49$ ($\text{CH}_2\text{Cl}_2/\text{MeOH} = 9:1$). $[\alpha]_{\text{D}}^{20} -2$ (c 1, CHCl_3). ^1H NMR (400 MHz, CDCl_3): δ 8.45 (d, 1H, $J = 7.7$ Hz), 7.86–7.84 (m, 1H), 7.74 (d, 1H, $J = 8.1$ Hz), 7.58 (d, 1H, $J = 7.1$ Hz), 7.51–7.41 (m, 3H), 6.83–6.78 (m, 3H), 6.12 (bt, 1H, $J = 5.7$ Hz), 4.37 (d, 2H, $J = 5.7$ Hz), 4.10 (q, 1H, $J = 6.6$ Hz), 3.76 (s, 3H), 3.23–3.20 (m, 1H), 2.90–2.85 (m, 1H), 2.14–1.95 (m, 3H), 1.89–1.69 (m, 4H), 1.47 (d, 3H, $J = 6.6$ Hz). ^{13}C NMR (100 MHz, CDCl_3): δ 175.2, 159.8, 140.7, 140.1, 134.0, 131.6, 129.6, 128.6, 127.2, 125.4, 125.3, 125.3, 124.5, 124.2, 119.8, 113.2, 112.7, 61.6, 55.1, 51.8, 49.1, 43.5, 43.2, 29.3, 18.6. IR (neat): 3293, 2937, 1644, 1263, 781 cm^{-1} . MS (EI): m/z 402 $[\text{M}]^+$. HRMS (EI), calcd for $\text{C}_{26}\text{H}_{30}\text{N}_2\text{O}_2$ 402.2307, found 402.2303.

1-[(R)-1-(1-Naphthyl)ethyl]-4-(4-methoxybenzylamino)carbonylpiperidine (15c). The title compound was obtained as described in compound **15a** in 88% yield (white amorphous solid). $R_f = 0.56$ ($\text{CH}_2\text{Cl}_2/\text{MeOH} = 9:1$). $[\alpha]_{\text{D}}^{20} -2$ (c 1, CHCl_3). ^1H NMR (400 MHz, CDCl_3): δ 8.45 (d, 1H, $J = 7.7$ Hz), 7.86–7.84 (m, 1H), 7.74 (d, 1H, $J = 8.1$ Hz), 7.57 (d, 1H, $J = 7.1$ Hz), 7.51–7.41 (m, 3H), 7.27 (d, 2H, $J = 8.5$ Hz), 6.84 (d, 2H, $J = 8.5$ Hz), 5.97 (bt, 1H, $J = 5.6$ Hz), 4.33 (d, 2H, $J = 5.6$ Hz), 4.10 (q, 1H, $J = 6.7$ Hz), 3.77 (s, 3H), 3.23–3.20 (m, 1H), 2.89–2.86 (m, 1H), 2.13–1.95 (m, 3H), 1.89–1.68 (m, 4H), 1.47 (d, 3H, $J = 6.7$ Hz). ^{13}C NMR (100 MHz, CDCl_3): δ 175.0, 158.9, 140.7, 134.0, 131.6, 130.5, 129.0, 128.6, 127.2, 125.4, 125.3, 125.3, 124.5, 124.2, 114.0, 61.6, 55.2, 51.8, 49.1, 43.5, 42.8, 29.3, 18.6. IR (neat): 3292, 2932, 1513, 1644, 1249, 781 cm^{-1} . MS (EI): m/z 402 $[\text{M}]^+$. HRMS (EI), calcd for $\text{C}_{26}\text{H}_{30}\text{N}_2\text{O}_2$ 402.2307, found 402.2299.

1-[(R)-1-(2-Naphthyl)ethyl]-4-(3-methoxybenzylamino)carbonylpiperidine (15d). The title compound was obtained as described in compound **15a** in 94% yield (white amorphous solid). $R_f = 0.43$ ($\text{CH}_2\text{Cl}_2/\text{MeOH} = 9:1$). $[\alpha]_{\text{D}}^{20} +10$ (c 1, CHCl_3). ^1H NMR (400 MHz, CDCl_3): δ 7.82–7.79 (m, 3H), 7.70 (s, 1H), 7.52 (dd, 1H, $J = 1.2$ and 8.4 Hz), 7.49–7.42 (m, 2H), 7.22 (t, 1H, $J = 7.6$ Hz), 6.83–6.79 (m, 3H), 5.95 (bt, 1H, $J = 5.7$ Hz), 4.38 (d, 2H, $J = 5.7$ Hz), 3.77 (s, 3H), 3.56 (q, 1H, $J = 6.7$ Hz), 3.16–3.14 (m, 1H), 2.90–2.88 (m, 1H), 2.11–1.91 (m, 3H), 1.89–1.70 (m, 4H), 1.44 (d, 3H, $J = 6.7$ Hz). ^{13}C NMR (100 MHz, CDCl_3): δ 175.0, 159.8, 141.7, 140.0, 133.2, 132.6, 129.6, 127.8, 127.7, 127.5, 125.9, 125.9, 125.8, 125.4, 119.8, 113.2, 112.8, 64.7, 55.1, 50.8, 49.7, 43.4, 43.2, 29.1, 19.3. IR (neat): 3296, 2932, 1645, 1264 cm^{-1} . MS (ESI): m/z 403 $[\text{M} + \text{H}]^+$. HRMS (ESI), calcd for $\text{C}_{26}\text{H}_{31}\text{N}_2\text{O}_2$ 403.2386, found 403.2390.

1-[(R)-1-(2-Naphthyl)ethyl]-4-(2-methoxybenzylamino)carbonylpiperidine (15e). The title compound was obtained as described in compound **15a** in 98% yield (white amorphous solid). $R_f = 0.47$ ($\text{CH}_2\text{Cl}_2/\text{MeOH} = 9:1$). $[\alpha]_D^{20} + 12$ (c 1, CHCl_3). $^1\text{H NMR}$ (400 MHz, CDCl_3): δ 7.82–7.79 (m, 3H), 7.70 (s, 1H), 7.51 (d, 1H, $J = 8.4$ Hz), 7.49–7.43 (m, 2H), 7.28–7.24 (m, 2H), 6.93–6.85 (m, 2H), 6.02 (bt, 1H, $J = 5.7$ Hz), 4.43 (d, 2H, $J = 5.7$ Hz), 3.84 (s, 3H), 3.57 (q, 1H, $J = 6.7$ Hz), 3.16–3.14 (m, 1H), 2.90–2.88 (m, 1H), 2.08–1.86 (m, 4H), 1.84–1.64 (m, 3H), 1.45 (d, 3H, $J = 6.7$ Hz). $^{13}\text{C NMR}$ (100 MHz, CDCl_3): δ 174.6, 157.5, 141.6, 133.2, 132.6, 129.7, 129.0, 128.8, 128.2, 127.8, 127.7, 127.5, 126.3, 126.0, 125.8, 125.4, 120.6, 110.2, 64.7, 55.2, 50.8, 49.8, 43.5, 39.2, 29.1, 19.3. IR (neat): 3306, 2933, 1645, 1243, 751 cm^{-1} . MS (ESI): m/z 403 $[\text{M} + \text{H}]^+$. HRMS (ESI), calcd for $\text{C}_{26}\text{H}_{31}\text{N}_2\text{O}_2$ 403.2386, found 403.2394.

1-[(S)-1-(2-Naphthyl)ethyl]-4-(3-methoxybenzylamino)carbonylpiperidine (15f). The title compound was obtained as described in compound **15a** in 83% yield (white amorphous solid). $R_f = 0.37$ ($\text{CH}_2\text{Cl}_2/\text{MeOH} = 9:1$). $[\alpha]_D^{20} - 10$ (c 1, CHCl_3). MS (ESI): m/z 403 $[\text{M} + \text{H}]^+$. HRMS (ESI), calcd for $\text{C}_{26}\text{H}_{31}\text{N}_2\text{O}_2$ 403.2386, found 403.2392.

1-[(R)-1-(1-Naphthyl)ethyl]-4-[3,4-(methylenedioxy)benzylamino]carbonylpiperidine (15g). The title compound was obtained as described in compound **15a** in 93% yield (white amorphous solid). $R_f = 0.47$ ($\text{CH}_2\text{Cl}_2/\text{MeOH} = 9:1$). $[\alpha]_D^{20} - 2$ (c 1, CHCl_3). $^1\text{H NMR}$ (400 MHz, CDCl_3): δ 8.45 (d, 1H, $J = 7.5$ Hz), 7.86–7.83 (m, 1H), 7.73 (d, 1H, $J = 8.1$ Hz), 7.56 (d, 1H, $J = 6.9$ Hz), 7.51–7.40 (m, 3H), 6.73–6.66 (m, 3H), 6.20 (bt, 1H, $J = 5.7$ Hz), 5.89 (s, 2H), 4.29 (d, 2H, $J = 5.7$ Hz), 4.08 (q, 1H, $J = 6.7$ Hz), 3.22–3.19 (m, 1H), 2.88–2.85 (m, 1H), 2.13–1.94 (m, 3H), 1.87–1.67 (m, 4H), 1.46 (d, 3H, $J = 6.7$ Hz). $^{13}\text{C NMR}$ (100 MHz, CDCl_3): δ 175.2, 147.8, 146.8, 140.7, 134.0, 132.4, 131.6, 128.6, 127.2, 125.4, 125.3, 125.3, 124.5, 124.2, 120.8, 108.2, 100.9, 61.6, 51.8, 49.1, 43.5, 43.0, 29.3, 18.6. IR (neat): 3294, 2924, 1644, 1489, 1252, 1040, 781 cm^{-1} . MS (ESI): m/z 417 $[\text{M} + \text{H}]^+$. HRMS (ESI), calcd for $\text{C}_{26}\text{H}_{29}\text{N}_2\text{O}_3$ 417.2178, found 417.2178.

1-[(S)-1-(1-Naphthyl)ethyl]-4-[3,4-(methylenedioxy)benzylamino]carbonylpiperidine (15h). The title compound was obtained as described in compound **15a** in 80% yield (white amorphous solid). $R_f = 0.56$ ($\text{CH}_2\text{Cl}_2/\text{MeOH} = 9:1$). $[\alpha]_D^{20} + 2$ (c 1, CHCl_3). MS (EI): m/z 417 $[\text{M} + \text{H}]^+$. HRMS (EI), calcd for $\text{C}_{26}\text{H}_{29}\text{N}_2\text{O}_3$ 417.2178, found 417.2173.

1-(1-Naphthylmethyl)-4-[3,4-(methylenedioxy)benzylamino]carbonylpiperidine (15i). The title compound was obtained as described in compound **15a** in >99% yield (white amorphous solid). $R_f = 0.48$ ($\text{CH}_2\text{Cl}_2/\text{MeOH} = 9:1$). $^1\text{H NMR}$ (400 MHz, CDCl_3): δ 8.30–8.28 (m, 1H), 7.84 (d, 1H, $J = 7.2$ Hz), 7.77 (d, 1H, $J = 7.8$ Hz), 7.52–7.45 (m, 2H), 7.41–7.37 (m, 2H), 6.74–6.67 (m, 3H), 5.91 (bm, 1H), 5.91 (s, 2H), 4.30 (d, 2H, $J = 5.7$ Hz), 3.87 (s, 2H), 2.99–2.96 (m, 2H), 2.35–2.29 (m, 1H), 2.18–2.01 (m, 3H), 1.88–1.72 (m, 3H). $^{13}\text{C NMR}$ (100 MHz, CDCl_3): δ 174.9, 147.8, 146.8, 134.1, 133.7, 132.5, 132.2, 128.3, 127.8, 127.2, 126.0, 125.6, 125.5, 125.0, 124.7, 120.9, 108.2, 101.0, 61.2, 53.3, 43.4, 43.1, 28.9. IR (neat): 3307, 2924, 1645, 1490, 1252, 1040 cm^{-1} . MS (ESI): m/z 403 $[\text{M} + \text{H}]^+$. HRMS (ESI), calcd for $\text{C}_{25}\text{H}_{27}\text{N}_2\text{O}_3$ 403.2022, found 403.2025.

1-(2-Naphthylmethyl)-4-[3,4-(methylenedioxy)benzylamino]carbonylpiperidine (15j). The title compound was obtained as described in compound **15a** in 88% yield (white amorphous solid). $R_f = 0.42$ ($\text{CH}_2\text{Cl}_2/\text{MeOH} = 9:1$). $^1\text{H NMR}$ (400 MHz, CDCl_3): δ 7.82–7.78 (m, 3H), 7.72 (s, 1H), 7.49–7.42 (m, 3H), 6.74–6.68 (m, 3H), 6.01 (t, 1H, $J = 5.6$ Hz), 5.91 (s, 2H), 4.31 (d, 2H, $J = 5.6$ Hz), 3.63 (s, 2H), 2.97–2.94 (m, 2H), 2.15–2.07 (m, 1H), 2.04–1.98 (m, 2H), 1.83–1.77 (m, 4H). $^{13}\text{C NMR}$ (100 MHz, CDCl_3): δ 174.9, 147.8, 146.8, 135.9, 132.7, 132.3, 127.8, 127.6, 127.6, 127.4, 127.3, 125.9, 125.5, 120.9, 108.2, 101.0, 63.2, 53.1, 43.3, 43.1, 28.9. IR (neat): 3293, 2923, 1643, 1490, 1252,

1040 cm^{-1} . MS (ESI): m/z 403 $[\text{M} + \text{H}]^+$. HRMS (ESI), calcd for $\text{C}_{25}\text{H}_{27}\text{N}_2\text{O}_3$ 403.2022, found 403.2025.

1-[1-Methyl-1-(1-naphthyl)ethyl]-4-[3,4-(methylenedioxy)benzylamino]carbonylpiperidine (15k). The title compound was obtained as described in compound **15a** in 90% yield (white amorphous solid). $R_f = 0.51$ (hexane/EtOAc = 1:1). $^1\text{H NMR}$ (400 MHz, CDCl_3): δ 9.56–9.53 (m, 1H), 7.82–7.79 (m, 1H), 7.72 (d, 1H, $J = 7.9$ Hz), 7.46–7.41 (m, 3H), 7.36 (t, 1H, $J = 7.6$ Hz), 6.73–6.71 (m, 2H), 6.67 (dd, 1H, $J = 1.1$ and 8.2 Hz), 6.00 (bt, 1H, $J = 5.7$ Hz), 5.90 (s, 2H), 4.29 (d, 2H, $J = 5.7$ Hz), 2.92 (bs, 2H), 2.21 (bm, 2H), 2.09–2.01 (m, 1H), 1.72 (bm, 4H), 1.56 (s, 6H). $^{13}\text{C NMR}$ (100 MHz, CDCl_3): δ 175.2, 147.8, 146.8, 144.0, 134.8, 132.4, 132.0, 128.5, 128.3, 127.9, 125.1, 124.7, 124.4, 123.5, 120.8, 108.2, 100.9, 62.3, 46.1, 44.0, 43.1, 29.8, 24.7. IR (neat): 3294, 2974, 1642, 1490, 1253, 1041, 780 cm^{-1} . MS (ESI): m/z 311 $[\text{M} + \text{H}]^+$. HRMS (ESI), calcd for $\text{C}_{27}\text{H}_{31}\text{N}_2\text{O}_3$ 431.2335, found 431.2330.

1-[1-(1-Naphthyl)ethyl]-4-tert-butoxycarbonylpiperazine (18). To a solution of *N*-Boc-piperazine **16** (107 mg, 0.58 mmol) and 1-acetonaphthone **17** (0.10 mL, 0.69 mmol) in MeOH/AcOH (50:1) (4 mL) was added sodium cyanoborohydride (38 mg, 0.58 mmol) at 0 °C. The mixture was allowed to stir for 48 h at 23 °C. The reaction was quenched with saturated NaHCO_3 solution, and the organic layer was extracted with CH_2Cl_2 . The organic layer was dried over Na_2SO_4 , filtered, and concentrated under reduced pressure. The residue was purified by silica gel column chromatography to furnish compound **18** (46 mg, 24%) as a colorless oil. $R_f = 0.75$ (hexane/EtOAc = 1:1). $^1\text{H NMR}$ (300 MHz, CDCl_3): δ 8.42 (d, 1H, $J = 7.2$ Hz), 7.86–7.83 (m, 1H), 7.74 (d, 1H, $J = 10.8$ Hz), 7.57 (d, 1H, $J = 7.2$ Hz), 7.50–7.39 (m, 3H), 4.09 (q, 1H, $J = 6.6$ Hz), 3.45–3.33 (m, 4H), 2.53 (bm, 2H), 2.42–2.35 (m, 2H), 1.47 (d, 3H, $J = 6.6$ Hz), 1.44 (s, 9H). $^{13}\text{C NMR}$ (75 MHz, CDCl_3): δ 154.7, 140.1, 134.0, 131.5, 128.7, 127.4, 125.5, 125.3, 125.3, 124.6, 124.0, 79.4, 61.5, 50.5, 43.8, 28.4, 18.7.

1-[1-(1-Naphthyl)ethyl]-4-(4-methoxybenzylamino)carbonylpiperazine (20). To a solution of Boc **18** (32 mg, 0.094 mmol) in dry CH_2Cl_2 (2 mL) was added trifluoroacetic acid (0.3 mL) at 0 °C. The mixture was allowed to stir for 1 h at 23 °C and then was concentrated under reduced pressure. To the residue was added toluene, and the mixture was concentrated under reduced pressure to give crude compound **19**. To a solution of 1,1'-carbonyldiimidazole (18.6 mg, 0.11 mmol) in dry CH_2Cl_2 (2 mL) was added dropwise 4-methoxybenzylamine **5c** (15.7 μL , 0.12 mmol) at 0 °C under argon atmosphere, and the mixture was allowed to stir for 4 h at 23 °C. The mixture was added dropwise to a solution of **19** in dry CH_2Cl_2 (1 mL). The mixture was allowed to stir for 24 h at 23 °C and then was concentrated under reduced pressure. The residue was purified by silica gel column chromatography to furnish compound **20** (34 mg, 90%) as a white amorphous solid. $R_f = 0.57$ ($\text{CH}_2\text{Cl}_2/\text{MeOH} = 9:1$). $^1\text{H NMR}$ (400 MHz, CDCl_3): δ 8.32 (d, 1H, $J = 7.5$ Hz), 7.81–7.78 (m, 1H), 7.69 (d, 1H, $J = 8.1$ Hz), 7.52 (d, 1H, $J = 7.1$ Hz), 7.44–7.36 (m, 3H), 7.13 (d, 2H, $J = 8.6$ Hz), 6.78 (d, 2H, $J = 8.6$ Hz), 4.22 (s, 2H), 4.07 (q, 1H, $J = 6.6$ Hz), 3.72 (s, 3H), 3.34–3.21 (m, 4H), 2.55–2.50 (m, 2H), 2.39–2.34 (m, 2H), 1.42 (d, 3H, $J = 6.6$ Hz). $^{13}\text{C NMR}$ (100 MHz, CDCl_3): δ 160.1, 160.0, 159.4, 141.1, 135.4, 132.9, 130.2, 130.1, 130.0, 128.9, 127.0, 126.8, 126.0, 125.2, 115.2, 62.6, 56.6, 51.7, 45.4, 45.2, 20.0. IR (neat): 3340, 2925, 1618, 1512, 1248 cm^{-1} . MS (ESI): m/z 404 $[\text{M} + \text{H}]^+$. HRMS (ESI), calcd for $\text{C}_{25}\text{H}_{30}\text{N}_2\text{O}_2$ 404.2338, found 404.2336.

Molecular Modeling. Computational analyses utilized the Sybyl 8.1 suite (Tripos, Inc.) and the GOLD docking program (CCDC) following previously described protocols.¹⁰

X-ray Crystallography. The complex of inhibitor **15g** with purified PLpro was formed prior to crystallization by incubating 10 mg/mL PLpro (in 20 mM Tris, pH 7.5, 10 mM DTT) with 2 mM **15g** at 4 °C for 16 h. Diffraction-quality crystals grew from a sitting drop containing 5 mg/mL PLpro, 1 mM **15g**, 1 M $(\text{NH}_4)_2\text{SO}_4$, 50 mM MES, pH 6.5, and 2.5% PEG 400. Crystals

were flash-frozen in liquid nitrogen and then transferred into a dry nitrogen stream at 100 K for X-ray data collection. The data set of the complex was collected at the Southeast Regional Collaborative Access Team (SER-CAT) beamline at the Advanced Photon Source, Argonne National Laboratory. Data were processed and scaled using the HKL2000 program suite. Crystals belonged to the space group C_2 , with two monomers in the asymmetric unit. The inhibitor-complexed structure was solved to 2.63 Å by molecular replacement using the SARS-CoV PLpro apoenzyme structure (PDB entry 2FE8) as a search model in the AMoRe program of the CCP4 suite. Manual model building was performed using Wincoot, and iterative rounds of positional and B -factor refinement and map building were performed using CNS. The structure was deposited under PDB code 3MJ5.

SARS-CoV Antiviral and PLpro Inhibition Assays. SARS-CoV antiviral assays and PLpro inhibition assays were performed as previously described.¹⁰

Acknowledgment. This work was supported by a National Institutes of Health Research Grant P01AI060915 (“Development of Novel Protease Inhibitors as SARS Therapeutics”). The authors gratefully acknowledge the synchrotron beamline personnel at Advanced Photon Source (SER-CAT) 22-ID and 22-BM beamlines. Use of the Advanced Photon Source was supported by the U.S. Department of Energy, Office of Science, Office of Basic Energy Sciences, under Contract No. W-31-109-Eng-38.

Supporting Information Available: HPLC and HRMS data of inhibitors. This material is available free of charge via the Internet at <http://pubs.acs.org>.

References

- (1) World Health Organization. Communicable Disease Surveillance & Response. http://www.who.int/csr/sars/archive/2003_05_07a/en and http://www.who.int/csr/sars/country/en/country2003_08_15.pdf.
- (2) Drosten, C.; Gunther, S.; Preiser, W.; van der Werf, S.; Brodt, H. R.; Becker, S.; Rabenau, H.; Panning, M.; Kolesnikova, L.; Fouchier, R. A.; Berger, A.; Burguiere, A. M.; Cinatl, J.; Eickmann, M.; Escriu, N.; Grywna, K.; Kramme, S.; Manuguerra, J. C.; Muller, S.; Rickerts, V.; Stürmer, M.; Vieth, S.; Klenk, H. D.; Osterhaus, A. D.; Schmitz, H.; Doerr, H. W. Identification of a novel coronavirus in patients with severe acute respiratory syndrome. *N. Engl. J. Med.* **2003**, *348*, 1967–1976.
- (3) (a) Ksiazek, T. G.; Erdman, D.; Goldsmith, C. S.; Zaki, S. R.; Peret, T.; Emery, S.; Tong, S.; Urbani, C.; Comer, J. A.; Lim, W.; Rollin, P. E.; Dowell, S. F.; Ling, A. E.; Humphrey, C. D.; Shieh, W. J.; Guarner, J.; Paddock, C. D.; Rota, P.; Fields, B.; DeRisi, J.; Yang, J. Y.; Cox, N.; Hughes, J. M.; LeDuc, J. W.; Bellini, W. J.; Anderson, L. J. A novel coronavirus associated with severe acute respiratory syndrome. *N. Engl. J. Med.* **2003**, *348*, 1953–1966. (b) Peiris, J. S.; Lai, S. T.; Poon, L. L.; Guan, Y.; Yam, L. Y. C.; Lim, W.; Nicholls, J.; Yee, W. K. S.; Yan, W. W.; Cheung, M. T.; Cheng, V. C.; Chan, K. H.; Tsang, D. N.; Yung, R. W. H.; Ng, T. K.; Yuen, K. Y. Coronavirus as a possible cause of severe acute respiratory syndrome. *Lancet* **2003**, *361*, 1319–1325.
- (4) Li, W.; Shi, Z.; Yu, M.; Ren, W.; Smith, C.; Epstein, J. H.; Wang, H.; Cramer, G.; Hu, Z.; Zhang, H.; Zhang, J.; McEachern, J.; Field, H.; Daszak, P.; Eaton, B. T.; Zhang, S.; Wang, L. F. Bats are natural reservoirs of SARS-like coronaviruses. *Science* **2005**, *310*, 676–679.
- (5) Lau, S. K. P.; Woo, P. C. Y.; Li, K. S. M.; Huang, Y.; Tsoi, H.-W.; Wong, B. H. L.; Wong, S. S. Y.; Leung, S. Y.; Chan, K.-H.; Yuen, K.-Y. Severe acute respiratory syndrome coronavirus-like virus in Chinese horseshoe bats. *Proc. Natl. Acad. Sci. U.S.A.* **2005**, *102*, 14040–14045.
- (6) He, J. F.; Peng, G.-W.; Min, J.; Yu, D.-W.; Liang, W.-J.; Zhang, S.-Y.; Xu, R.-H.; Zheng, H.-Y.; Wu, X.-W.; Xu, J.; Wang, Z.-H.; Fang, L.; Zhang, X.; Li, H.; Yan, X.-G.; Lu, J.-H.; Hu, Z.-H.; Huang, J.-C.; Wan, Z.-Y.; Hou, J.-L.; Lin, J.-Y.; Song, H.-D.; Wang, S.-Y.; Zhou, X.-J.; Zhang, G.-W.; Gu, B.-W.; Zheng, H.-J.; Zhang, X.-L.; He, M.; Zheng, K.; Wang, B.-F.; Fu, G.; Wang, X.-N.; Chen, S.-J.; Chen, Z.; Hao, P.; Tang, H.; Ren, S.-X.; Zhong, Y.; Guo, Z.-M.; Liu, Q.; Miao, Y.-G.; Kong, X.-Y.; He, W.-Z.; Li, Y.-X.; Wu, C.-I.; Zhao, G.-P.; Chi, R. W. K.; Chim, S. S. C.; Tong, Y.-K.; Chan, P. K. S.; Tam, J. S.; Lo, Y. M. D. Molecular evolution of the SARS-coronavirus during the course of the SARS epidemic in China. *Science* **2004**, *303*, 1666–1669.
- (7) Baker, S. C. Coronaviruses: Molecular Biology. In *Encyclopedia of Virology*, 3rd ed.; Mahy, B. W. J., Van Regenmortel, M. H. V., Eds.; Academic Press: Amsterdam, 2008; Vol. 1, pp 554–562.
- (8) Ghosh, A. K.; Xi, K.; Johnson, M. E.; Baker, S. C.; Mesecar, A. D. Progress in anti-SARS coronavirus chemistry, biology and chemotherapy. *Annu. Rep. Med. Chem.* **2006**, *41*, 183–196. (b) Yang, H.; Bartlam, M.; Rao, Z. Drug design targeting the main protease, the Achilles' heel of coronaviruses. *Curr. Pharm. Des.* **2006**, *12*, 4573–4590.
- (9) (a) Ghosh, A. K.; Xi, K.; Grum-Tokars, V.; Xu, X.; Ratia, K.; Fu, W.; Houser, K. V.; Baker, S. C.; Johnson, M. E.; Mesecar, A. D. Structure-based design, synthesis, and biological evaluation of peptidomimetic SARS-CoV 3CLpro inhibitors. *Bioorg. Med. Chem. Lett.* **2007**, *17*, 5876–5880. (b) Jain, R. P.; Pettersson, H. I.; Zhang, J.; Aull, K. D.; Fortin, P. D.; Huitema, C.; Eltis, L. D.; Parrish, J. C.; James, M. N. G.; Wishart, D. S.; Vederas, J. C. Synthesis and evaluation of keto-glutamine analogues as potent inhibitors of severe acute respiratory syndrome 3CLpro. *J. Med. Chem.* **2004**, *47*, 6113–6434. (c) Vederas, J. C.; Jain, R. P. Structural variations in keto-glutamines for improved inhibition against hepatitis A virus 3C proteinase. *Bioorg. Med. Chem. Lett.* **2004**, *14*, 3655.
- (10) (a) Ratia, K.; Pegan, S.; Takayama, J.; Sleeman, K.; Coughlin, M.; Chaudhuri, R.; Fu, W.; Prabhakar, B. S.; Johnson, M. E.; Baker, S. C.; Ghosh, A. K.; Mesecar, A. D. A noncovalent class of papain-like protease/deubiquitinase inhibitors blocks SARS virus replication. *Proc. Natl. Acad. Sci. U.S.A.* **2008**, *105*, 16119–16124. (b) Ghosh, A. K.; Takayama, J.; Aubin, Y.; Ratia, K.; Chaudhuri, R.; Baez, Y.; Sleeman, K.; Coughlin, M.; Nichols, D. B.; Mulhearn, D. C.; Prabhakar, B. S.; Baker, S. C.; Johnson, M. E.; Mesecar, A. D. Structure-based design, synthesis, and biological evaluation of a series of novel and reversible inhibitors for the severe acute respiratory syndrome-coronavirus papain-like protease. *J. Med. Chem.* **2009**, *52*, 5228–5240.
- (11) (a) Devaraj, S. G.; Wang, N.; Chen, Z.; Chen, Z.; Tseng, M.; Barretto, N.; Lin, R.; Peters, C. J.; Tseng, C.-T. K.; Baker, S. C.; Li, K. Regulation of IRF-3-dependent innate immunity by the papain-like protease domain of the severe acute respiratory syndrome coronavirus. *J. Biol. Chem.* **2007**, *282*, 32208–32211. (b) Ratia, K.; Saikatendu, K. S.; Santarsiero, B. D.; Barretto, N.; Baker, S. C.; Stevens, R. C.; Mesecar, A. D. Severe acute respiratory syndrome coronavirus papain-like protease: structure of a viral deubiquitinating enzyme. *Proc. Natl. Acad. Sci. U.S.A.* **2006**, *103*, 5717–5722. (c) Barretto, N.; Jukneliene, D.; Ratia, K.; Chen, Z.; Mesecar, A. D.; Baker, S. C. The papain-like protease of severe acute respiratory syndrome coronavirus has deubiquitinating activity. *J. Virol.* **2005**, *79*, 15189–15198.
- (12) (a) Lindner, H. A.; Fotouhi-Ardakani, N.; Lytvyn, V.; Lachance, P.; Sulea, T.; Ménard, R. The papain-like protease from the severe acute respiratory syndrome coronavirus is a deubiquitinating enzyme. *J. Virol.* **2005**, *79*, 15199–15208. (b) Sulea, T.; Lindner, H. A.; Purisima, E. O.; Ménard, R. Deubiquitination, a new function of the severe acute respiratory syndrome coronavirus papain-like protease? *J. Virol.* **2005**, *79*, 4550–4551.
- (13) Ziebuhr, J.; Schelle, B.; Karl, N.; Minskaia, E.; Bayer, S.; Siddell, S. G.; Gorbalenya, A. E.; Thiel, V. Human coronavirus 229E papain-like proteases have overlapping specificities but distinct functions in viral replication. *J. Virol.* **2007**, *81*, 3922–3932.
- (14) Oba, M.; Tanaka, M.; Takano, Y.; Suemune, H. Concise synthetic strategy toward cyclic α -disubstituted α -amino acids bearing a δ -nitrogen atom: chiral 1-substituted 4-aminopiperidine-4-carboxylic acids. *Tetrahedron* **2005**, *61*, 593–598.
- (15) Gaspari, P.; Banerjee, T.; Malachowski, W. P.; Muller, A. J.; Prendergast, G. C.; DuHadaway, J.; Bennett, S.; Donovan, A. M. Structure–activity study of brassinin derivatives as indoleamine 2,3-dioxygenase inhibitors. *J. Med. Chem.* **2006**, *49*, 684–692.
- (16) Dolby, L. D.; Biere, H. The total synthesis of (\pm)-epidasycarpidone and (\pm)-epiuleine. *J. Org. Chem.* **1970**, *35*, 3843–3845.
- (17) Yang, Q.; Ney, J. E.; Wolfe, J. P. Palladium-catalyzed tandem N-arylation/carboamination reactions for the stereoselective synthesis of N-aryl-2-benzyl pyrrolidines. *Org. Lett.* **2005**, *7*, 2575–2578.
- (18) Tahtaoui, C.; Parrot, I.; Klotz, P.; Guillier, F.; Galzi, J.-L.; Hibert, M.; Ilien, B. Fluorescent pirenzepine derivatives as potential

- bitopic ligands of the human M1 muscarinic receptor. *J. Med. Chem.* **2004**, *47*, 4300–4315.
- (19) Matsuno, K.; Ichimura, M.; Nakajima, T.; Tahara, K.; Fujiwara, S.; Kase, H.; Ushiki, J.; Giese, N. A.; Pandey, A.; Scarborough, R. M.; Lokker, N. A.; Yu, J.-C.; Irie, J.; Tsukuda, E.; Ide, S.; Oda, S.; Nomoto, Y. Potent and selective inhibitors of platelet-derived growth factor receptor phosphorylation. 1. Synthesis, structure–activity relationship, and biological effects of a new class of quinazoline derivatives. *J. Med. Chem.* **2002**, *45*, 3057–3066.